NASA CONTRACTOR REPORT 159209

NASA-CR-159209
19800013945

ANALYSIS OF NASA JP-4 FIRE TESTS DATA AND DEVELOPMENT OF A SIMPLE FIRE MODEL

PHANI RAJ

ARTHUR D. LITTLE, INC.
CAMBRIDGE, MA. 02140
C-81857

NASA CONTRACT NAS1-15380
APRIL, 1980

National Aeronautics and Space Administration

Langley Research Center
Hampton, Virginia 23665
AC 804 827-3966

PREFACE

The analysis presented in this report was performed as a part of the overall effort conducted by Arthur D. Little, Inc. on behalf of NASA to assess the risks posed by the use of carbon fiber composite materials in commercial aircraft. This risk study was performed under the direction of Dr. A. S. Kalelkar. The JP-4 fire analysis presented in this report was performed by Dr. P. K. Raj.

We express our sincere thanks to Dr. J. Mansfield of NASA Ames Research Center who provided the encouragement and the technical critique of the work. Our thanks are also due to Mr. L. Linley and Mr. D. Pippen at NASA, White Sands Test Facility, who provided the fire test data and answered numerous questions on the experimental details. We wish to express our appreciation of the careful review performed by Dr. W. Elber of NASA, Langley.

TABLE OF CONTENTS

LIST OF TABLES

LIST OF FIGURES

Summary

National Aeronautics and Space Administration (NASA) conducted a series of large scale pool fire tests involving 7.5m and 15m diameter JP-4 fires. Temperature, velocity and specie concentrations were measured within the fire at several height locations and at radial positions. The peak temperature recorded in the fire was in the 1500 K - 1550 K range, velocity of gases in the 11 to 12 m/s (at 6m height in the 15m diameter fire). The oxygen to nitrogen mass ratio along the centerline of the fire was seen to be about 0.05 and almost constant with height. One of the important observations made in the experiments was the significant reduction ("necking") in the fire diameter very close to the base.

A theoretical model has been formulated. The model is based on air entrainment into the fire plume and its partial combustion. Analytical solutions to the model equations have been derived. The two free parameters in the model are the entrainment coefficient and the air mixedness factor. The results of the model agree exceedingly well, qualitatively with both temperature data and the velocity data. Quantitative agreement is achieved by suitably adjusting the values of the entrainment coefficient and the mixedness factor. These values are respectively 0.15 and 0.45. The entrainment coefficient value is well within the range of values reported in the literature for other plumes. The model also predicts the necking of the fire.

The specie composition data obtained in the experiments have not been compared to model predictions because the model formulation does not take into account the detailed chemistry of combustion.

1. INTRODUCTION

1.1 BACKGROUND

Turbulent fires have been the subject of research and inquiry for several decades now because of the importance of large controlled fires in industrial processes and their effect on the design of furnaces and boilers. While the understanding of controlled fires has been significant, the knowledge related to uncontrolled combustion of fuels (such as may occur from the spill and ignition of oil from a storage tank or from the spill and ignition of jet fuel subsequent to an aircraft crash) is limited. Many researchers have attempted to model the behavior of large turbulent fires in the atmosphere; the end results sought in the models vary depending on their application. For example, to evaluate hazards to structures and people outside the fire, the radiant heat emission is of interest -- many models deal with this. To evaluate heat transfer to structures engulfed in the fire, it is necessary to know the temperature distribution, the flow field and turbulence level within the fire. Theoretical models, currently available in the literature to characterize turbulent fires, treat only very simple cases. These models, in many cases, are supplemented by empirical results.

Theoretical models describing turbulent fires in the open range from very simple models to very complicated numerical models. Thomas (1962) has presented a very simple approach to determining the visible flame height of a turbulent fire. This model is based almost totally on dimensional analyses and the single constant in the equation for flame height has been evaluated experimentally. However, the model does not give the details of either the temperature field or the velocity field in the fire. A somewhat more complicated model which gives the mean velocity and temperature field within a fire has been proposed by Steward (1970). More elaborate formulations are based on considering the details of turbulent mixing, chemical reactions within the fire. Because of the complexities in the equations, the solutions are based on numerical techniques (see Nielson and Tao, 1965 and Harsha et al., 1978).

The fundamental limitation common to all of the models is the lack of data from large scale fires, especially such data as the temperature, velocity, and chemical specie distributions from within the fire. Many of the model predictions have been tested with small, laboratory scale fires; however, it is uncertain whether the scale effects have been properly modelled in the theoretical formulations. Experimental determination of chemical specie concentrations within a turbulent fire has been attempted only recently by Alger et al. (1979).

The knowledge of the distributions of velocity, temperature and oxygen concentration within a large fire is important to evaluate certain kinds of problems. One of these problems is the determination of the extent of oxidation of small fibers of carbon during their flight through a fire. The problem is of interest to NASA because of the need to assess the risks posed by the burning of carbon fiber composite structures in large fuel fires. The details of the carbon fiber problem and the release scenarios are described in recent reports by NASA (1979). Because of the importance of the need to obtain quantitative estimates for the amount of single carbon fibers released from the burning of a composite material in a large fire and because there were no experimental data indicating the variations in the chemical compositions within a large fire, NASA undertook a large-scale experimental program.

In this experimental program measurements of temperature and chemical compositions were made at various locations within large turbulent pool fires of JP-4 fuel. Two pool diameters were used, namely, 7.62 m (25 ft) and 15.24 m (50 ft). In most of the tests, the vertical gas velocity was also recorded at one particular height above the pool. The objective of the tests was to gather data as well as to fine tune a numerical model incorporating the values of parameters obtained from the field data and thus provide a method for predicting the oxidation of carbon fibers.

Arthur D. Little, Inc., (ADL), under contract to NASA, designed, fabricated, and installed a high temperature anemometer for measurements of gas velocities in the fire. Also ADL was contracted to participate in all of the field experiments and provide an independent evaluation of the data using simplified models, wherever possible. This report deals with the development of a simplified turbulent fire model, analysis of the data, and the conclusions. Because of the financial and time constraints, the investigation is limited to simplified analyses.

1.2 OBJECTIVES

The objectives of the work performed by Arthur D. Little included:

- measuring the gas velocities in a large turbulent fire, and
- analyzing (using simplified methods) the experimental data.

1.3 SCOPE OF WORK

In order to achieve the above objective, the scope of work performed included:

- Design, fabrication, and installation of a high-temperature anemometer to measure the vertical velocity of the hot gases within the fire.
- Development of a simple turbulent fire model to provide unified scaling correlations. Also to develop simple formulae for the conditions under which substantial reduction ("necking") in the fire diameter was possible.
- Analysis of the experimental data on temperature and velocity, using the simple model developed.
- Review of data from other experiments and comparisons with the NASA experimental data.

The design details and the calibration of the high temperature velocity meter are discussed in Chapter 2. Also indicated are the velocities measured in two different fires. The development of a simple turbulent fire model is indicated in Chapter 3. Correlations are obtained for the necking of the fire and the location of the minimum

cross section. Also expressions are given for mean temperature, velocity, and gas density at different cross sections. The Froude number scaling of fires is clearly demonstrated. In Chapter 4 the data obtained from the series of tests conducted by NASA are reviewed and compared with the model predictions. Also the limited information from the literature is used for comparison with the NASA data. General observations and conclusions are given.

2. DESIGN AND USE OF HIGH TEMPERATURE ANEMOMETER

The measurement of velocities of hot gases within the combustion zone of a turbulent fire is an extremely difficult operation because of the high temperature and the very high heat loading on the instrument. However, by providing adequate water cooling for the measuring instrument, it can be protected. This is the principle on which our design of an anemometer for use in a fire environment is based.

2.1 INSTRUMENT DESIGN

The design of the fan anemometer is shown in Figure 2.1. It consists of a 4-blade impeller mounted on a shaft on ball bearings. The impeller blades are made of TD Nickel Chrome (supplied by NASA, Langley Research Center), and welded on to the shaft with stainless steel welds. The rotational speed of the shaft is measured electrically (described below) using a disc and an optical switch. The entire housing including the bearing assemblies, and the electronic speed measuring devices is water cooled by circulating water in 0.6 cm diameter (1/4") copper tubes.

Details of the electronics for the anemometer sensor are shown in Figure 2.2. A spectronics Optical Switch type 1874-4 is mounted inside the water-cooled cavity of the fan anemometer. This optical switch consists of a Light Emitting Diode (LED) facing a phototransistor. The LED radiation output to the phototransistor is interrupted once every revolution of the fan shaft by a 180°-sectored disc mounted on this shaft. The change in radiation received by the phototransistor is transformed into a voltage which is applied to the input of OP AMP IC1.

OP AMP IC2 reverses the polarity of IC1 output, and the resulting pulse triggers IC3, a 555 timer, whose output pulse is approximately 11 msec. The duration of this pulse is constant, but the time OFF between pulses is a function of the shaft RPM. The pulses are then integrated by an R-C network, and the resulting DC voltage is available at the output.

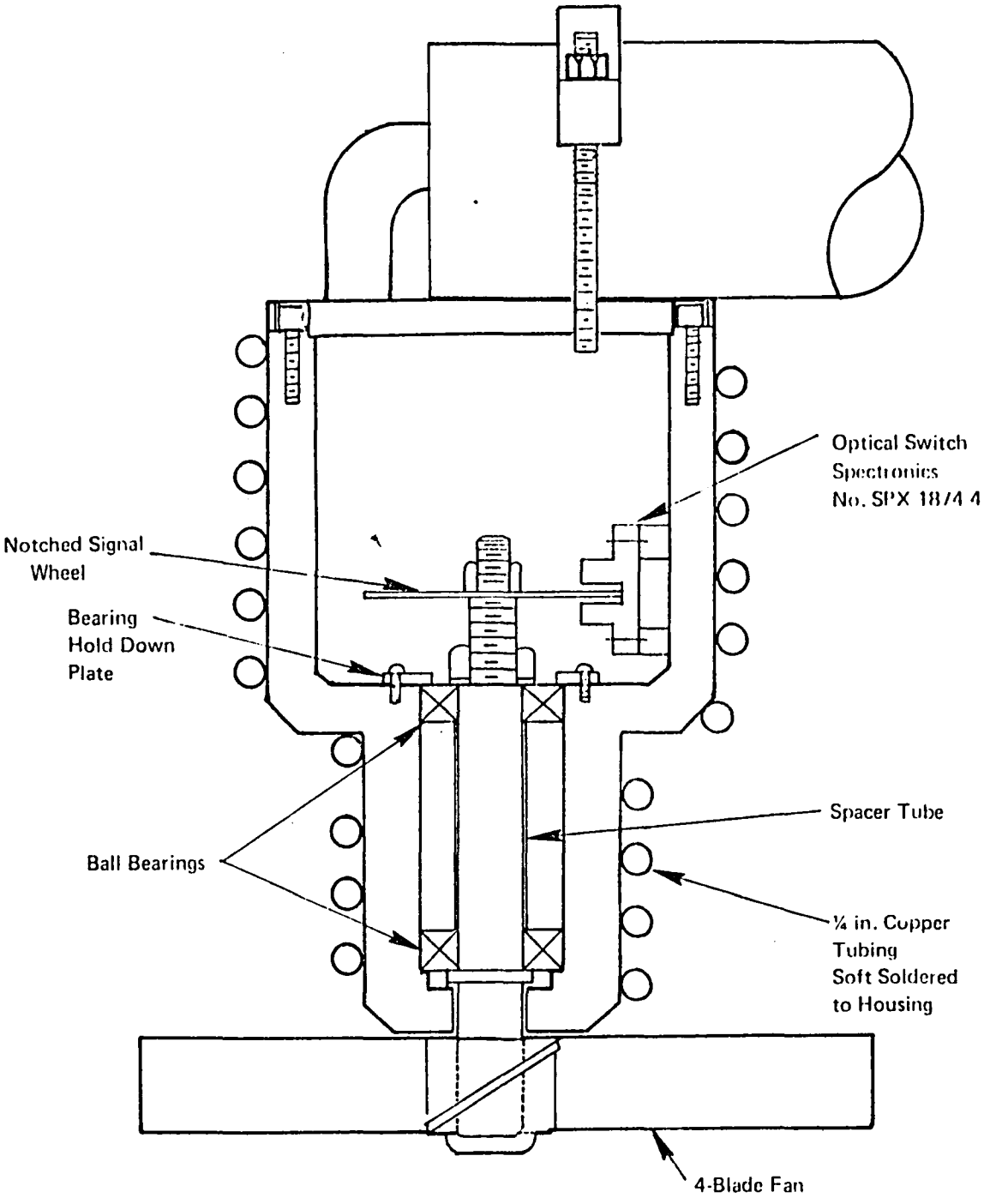

FIGURE 2.1 FAN ANEMOMETER ASSEMBLY

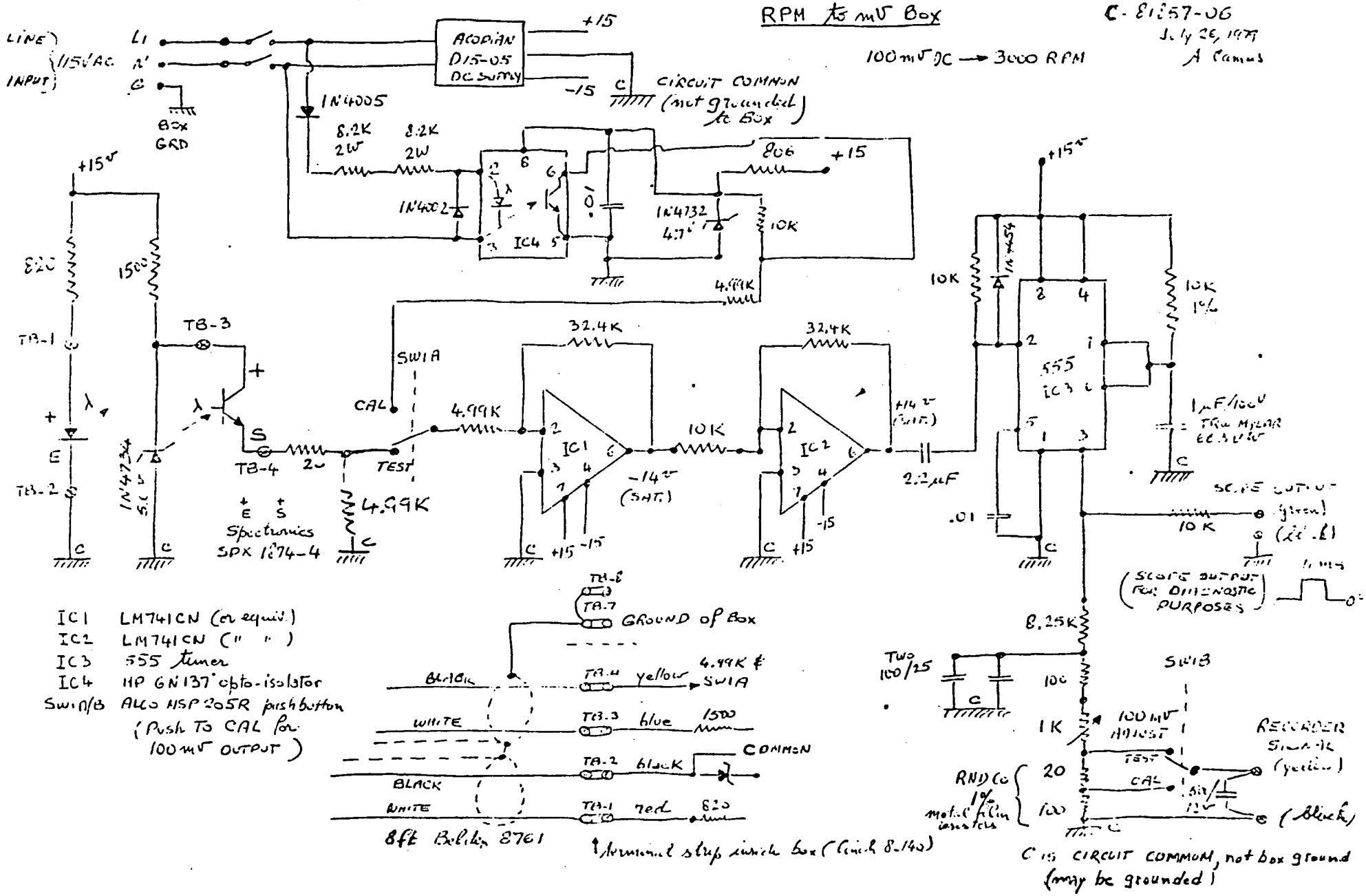

FIGURE 2.2: SCHEMATIC DIAGRAM FOR FAN ANEMOMETER ELECTRONICS

Opto Isolater IC4 delivers pulses from the line voltage to OP AMP IC1 when the CAL pushbutton switch is depressed, and the output, taken across 100 ohm, is adjusted to 100 mV with the CAL pot mounted on the front panel. This output corresponds to a 3600 RPM signal across a 100 ohm resistor. On TEST position, the output is taken across a 120 ohm resistor network so that a 100 mV output corresponds to a shaft speed of 3,000 rpm.

2.2 CALIBRATION OF THE INSTRUMENT

The anemometer was calibrated at ambient temperature in a wind tunnel at Harvard University. The wind tunnel test section consisted of a throat 70 x 100 cm. Wind speeds up to 20 m/s were used. The calibration output obtained at different free stream velocities is indicated in Figure 2.3. It is seen that the response of the instrument is linear over the 0 to 20 m/s range and can be expressed by the simple relationship:

$$U = 0.1143\ V \qquad (2.1)$$

where:

U = free stream gas velocity (m/s)

V = voltage output from the anemometer (mV)

It is noted that the calibration was performed at ambient temperature ($\simeq$ 290 K). When this anemometer is used in a high temperature gas environment, the above calibration may not give an accurate value for the gas velocity because of the decreased gas density. However, it can be shown (see Appendix A) that the effect of a free stream gas density variation on the anemometer calibration is very small. It can also be shown that in a high temperature gas environment, to get the actual gas velocity from the measured voltage output, the value of velocity obtained by using Equation 2.1 has to be increased. It is estimated that in a 1500 K environment, the above correction is about 13% for U = 3.3 m/s and about 3% at U = 16 m/s.

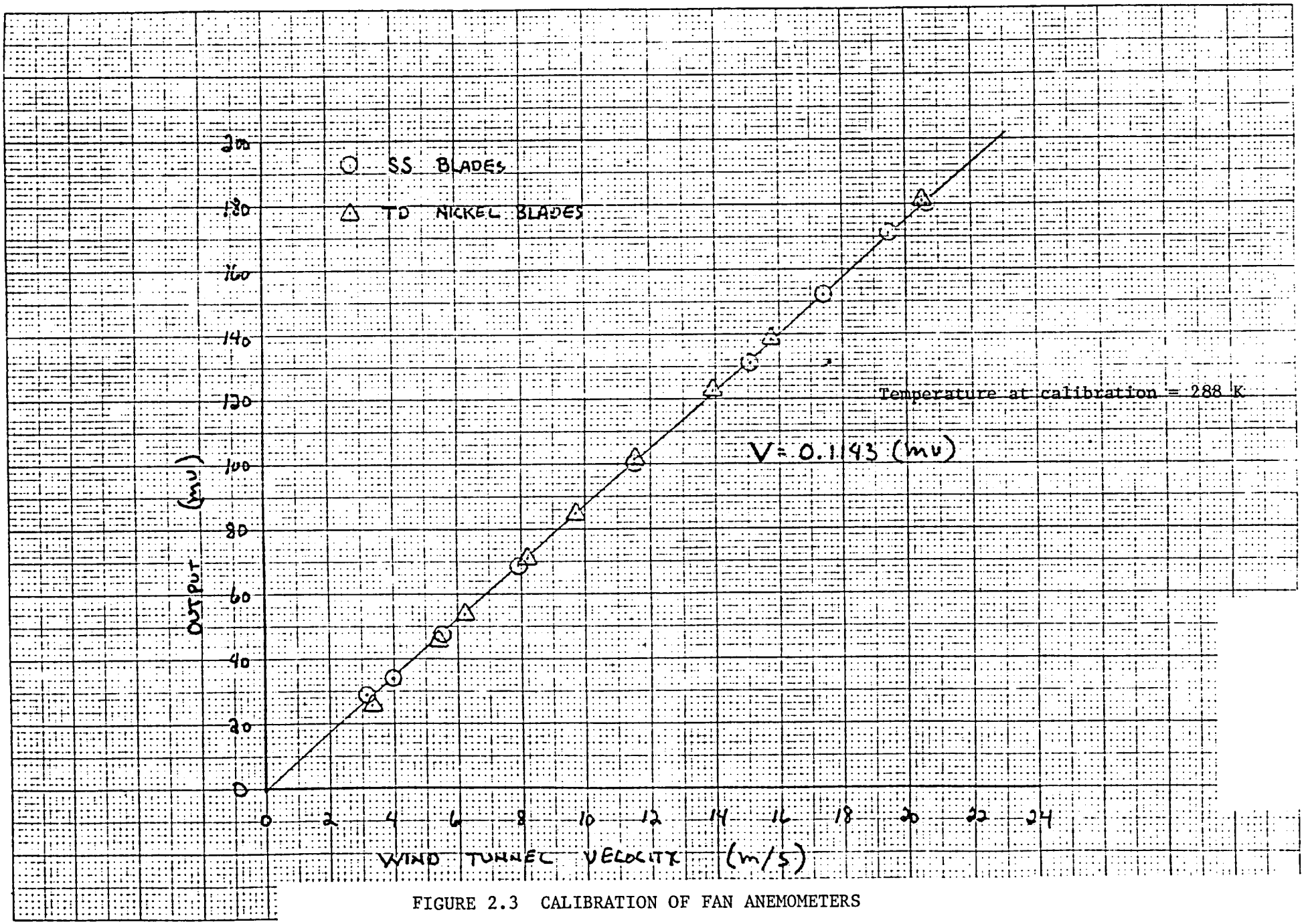

FIGURE 2.3 CALIBRATION OF FAN ANEMOMETERS

The time constant for the fan anemometer is estimated to be 50 seconds.

2.3 USE IN THE EXPERIMENT

The instrument was used in a vertical axis position to measure the vertical component of the velocity of gases. It was located at (18.8 ft) 5.7 m above the ground and on the vertical centerline. The anemometer was positioned with the impellers facing the pool. The signals from the anemometer were recorded on a strip chart recorder.

Typical velocity records obtained in the two experiments (#5 and #6) with 50 ft diameter fires are illustrated in Figures 2.4a and 2.4b, respectively. It is seen that in both experiments the instrument worked for a relatively short period of time compared to the duration of the fire. For example, in test #5 (Figure 2.4a) velocity measurements could be made only for 2 minutes in a 6-minute fire.

The velocity indicated (Figure 2.4a) reaches a maximum value in about 50s, remains steady for about 2 minutes. Subsequently the record shows a falling velocity. This is attributed to the seizure in the bearings of the instrument caused by the intense heat.* The steady value of about 100 mV indicated is probably a good indication of the true velocity of the hot gases. However, it should be noted that due to the uncertainty in the measurement, caused perhaps by the bearing friction, the recorded velocities may not be very accurate.

2.4 RESULTS

The velocity results obtained in two different experiments are shown in Table 2.1. It is seen that the velocity measured (estimated) is about 11.5 m/s (mean value) with a fluctuation of $\pm$ 0.5 m/s, in all of the experiments.

2.5 CONCLUSIONS

From this initial test with the ADL fan anemometer, we can draw the following conclusions:

1. The concept of the fan anemometer was proved successful.
2. The anemometer measured a velocity of approximately 11.5 m/s (37.7 ft/sec) at a height of 20 feet within the central core of a 50-foot

---

* A later test in the lab which simulated the above problem by heating the fan and the shaft with a blow torch indicated the same kind of seizure and binding in rotation.

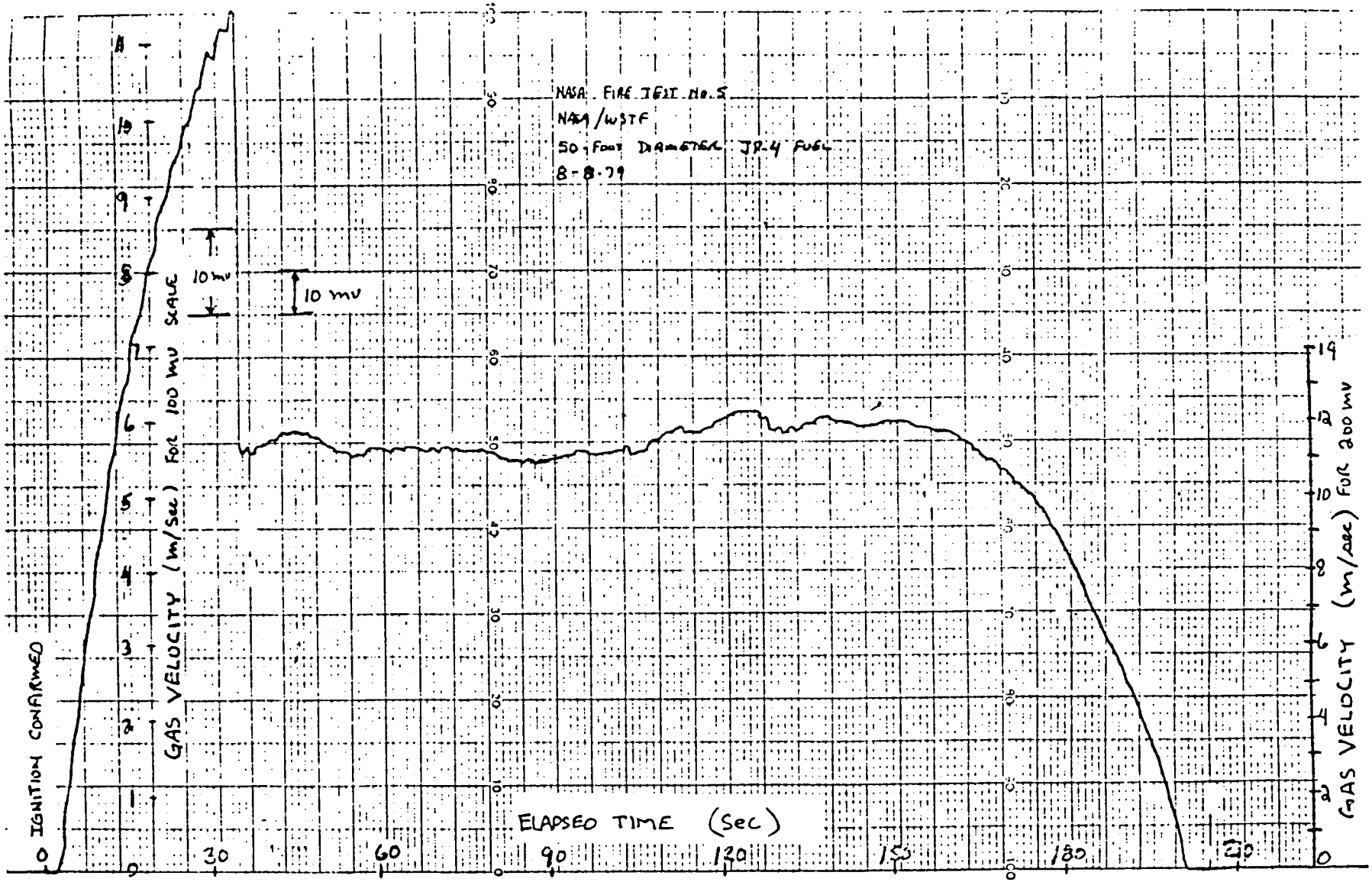

FIGURE 2.4a: VELOCITY DATA FROM NASA 50-FOOT DIAMETER FIRE NO. 5

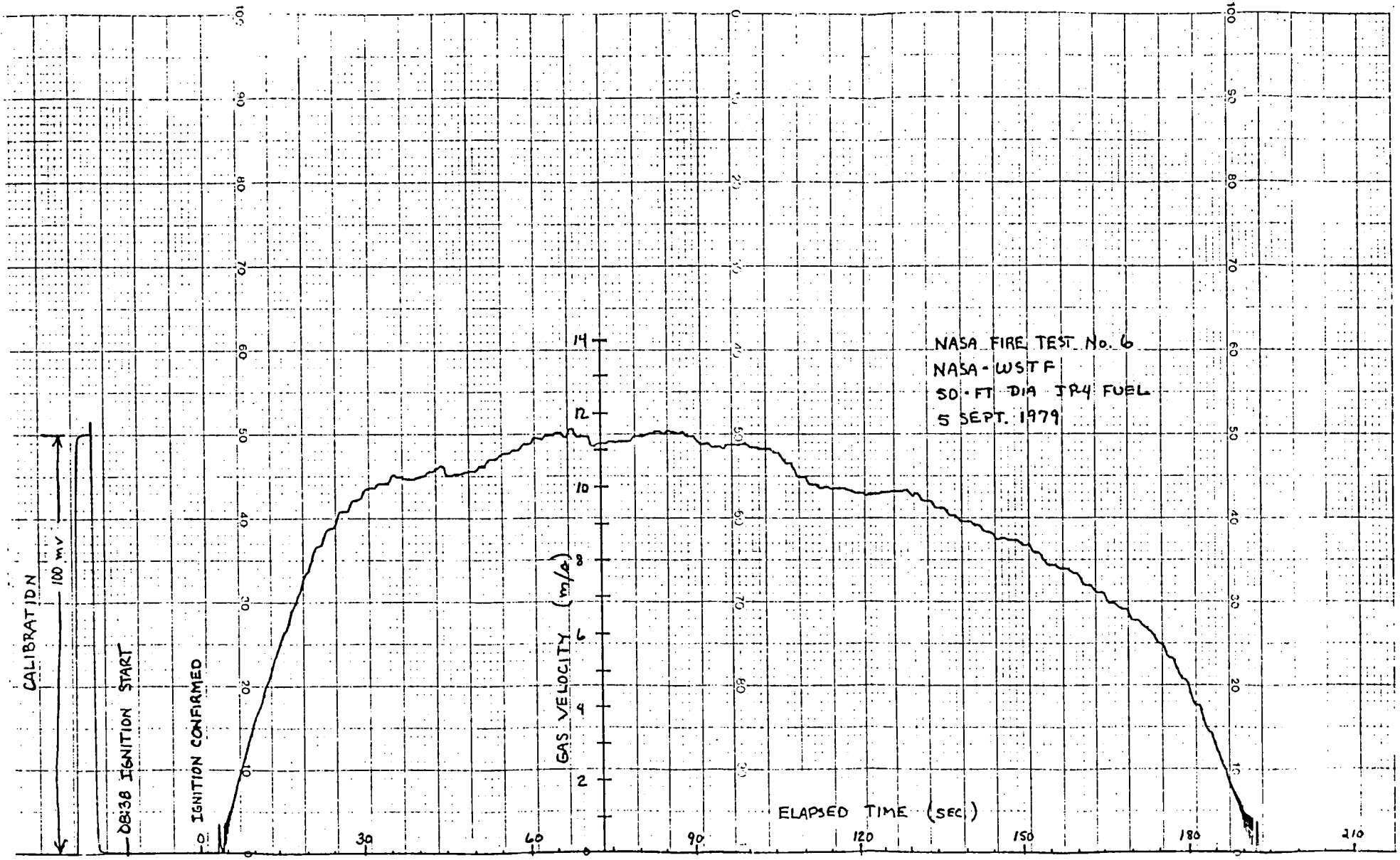

FIGURE 2.4b: VELOCITY DATA FROM NASA/WSTF 50-FOOT DIAMETER FIRE NO. 6 .

TABLE 2.1

RESULTS FROM VELOCITY MEASUREMENTS

Test #	Date	Diameter of Fire (m)	Measured Anemometer Output Voltage-Mean Value Under Steady Conditions (milli V)	Measured Mean Temperature at the Instrument Location (K)	Estimated Mean Velocity* (m/s)	Variations in Measured Gas Velocity† (m/s)
5	8/8	15.2	95	1230 ± 40	10.9	±0.6
6	7/13	15.2	100	1350 ± 40	11.5	$\pm \begin{matrix} 0.7 \\ 0.6 \end{matrix}$

* Using Equation 2.1

† Maximum deviations

diameter JP-4 jet fuel fire. The flame velocity was constant throughout the portion of the test where the anemometer was operable. It is, however, noted that the measurements may be approximate because of the bearing seizure problem noted earlier.

3. Mechanical interference in the sensor head of the anemometer caused the unit to stop operating after 160 seconds.

3. SIMPLIFIED TURBULENT FLAME MODEL

3.1 INTRODUCTION

In this chapter a simple model is formulated for a turbulent fire, the main aim of which is to evaluate the velocity and temperature variables with height above the fuel pool. This model is essentially the same as that formulated by Steward (1972); however, certain omissions in Steward's model have been corrected and in addition, the unmixedness of air with fuel vapors is explicitly taken into account. Also closed form expressions for certain specific properties of interest are indicated. Results for the variation of physical quantities such as velocity, temperature, and fire plume radius with height are indicated. A specific example has also been worked out.

3.2 PHYSICAL CONCEPTS ON WHICH THE MODEL IS BASED

Consider a circular pool fire (turbulent) burning steadily in an open atmosphere. This situation is illustrated schematically in Figure 3.1. The fuel vapors generated by the boiling of the liquid pool, entrain a certain amount of air, close to the bottom of the fire. This air and fuel mixture burns (probably close to the outer surface of the visible plume) and heats up the as-yet-rich fuel vapor. This additional heat input creates increased buoyancy of vapors which, therefore, accelerate in the vertical direction. Because of the increased velocity a larger mass of air is now entrained from the environment. This additional air again combusts with fuel vapor to generate additional buoyancy. This process continues until all of the fuel vapors released at the fuel surface are burned. The consequences of the above processes are that the upward velocity of the gases increases continuously up to the height over which a stoichiometric amount of air is entrained. Also, the temperature of the mixture of fuel and burned gases increases continuously with height up to the stoichiometric height. Above this height there is no more fuel to burn, but because the gases are hot, they rise and continue to entrain air and cool off. Therefore, the entire process

of combustion, upward acceleration and air entrainment can be represented mathematically by the equations of continuity, entrainment, momentum and energy. The analysis is indicated below.

3.3 MODEL FORMULATION

Considering a section at height z above the pool and another section at z + dz (Figure 3.2). We write the conservative equations of mass momentum and energy to the fluid passing through these sections. The following assumptions are made:

- flow is steady;
- velocity, density, temperature, etc., are uniform across the section ("top hat profile");
- gases are all perfect gases;
- the molar specific heats of air, burnt gas and the fuel vapor are identical;
- the fire is circular and is not bent by any wind effects.

Mass Conservation *

$$\frac{d}{dz}(u \rho \pi y^2) = \alpha \left(\frac{\rho}{\rho_a}\right)^{1/2} u \rho_a 2\pi y \qquad (3.1)$$

Rate of increase of mass flux over dz

$\alpha \left(\frac{\rho}{\rho_a}\right)^{1/2}$: effective entrainment coefficient

$u \rho_a 2\pi y$: Total air entrainment rate

Momentum Conservation

$$\frac{d}{dz}(u^2 \rho \pi y^2) = g(\rho_a - \rho) \pi y^2 \qquad (3.2)$$

Rate of increase of momentum flux over dz

Buoyancy force

* All symbols are defined in the nomenclature.

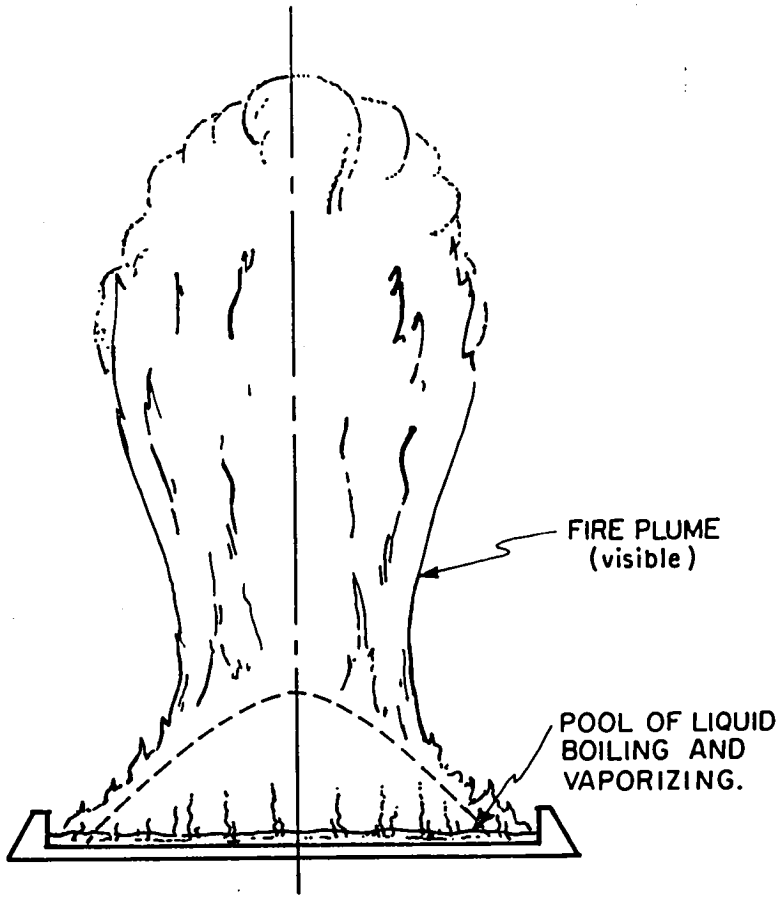

FIGURE 3.1. SCHEMATIC DIAGRAM SHOWING THE TURBULENT FIRE ON A POOL OF FLAMMABLE LIQUID

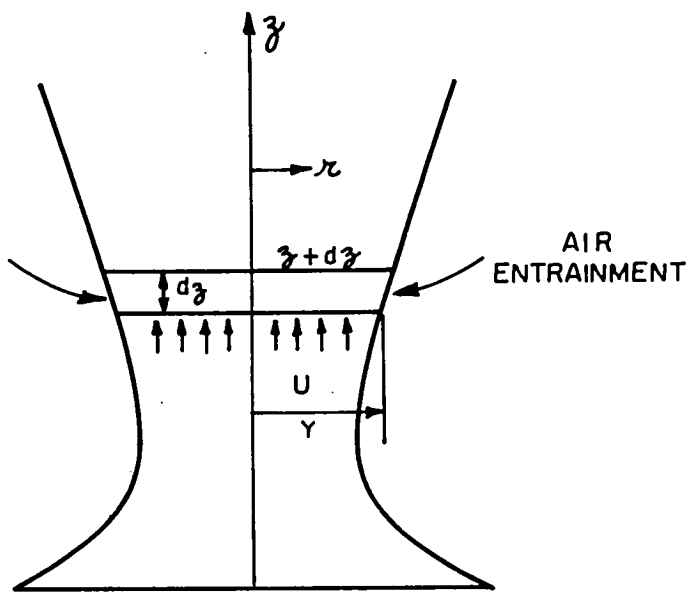

FIGURE 3.2. SCHEMATIC DIAGRAM INDICATING THE CONTROL VOLUME FOR THE THEORETICAL MODEL

Energy Equation

$$\frac{d}{dz}(u\rho\pi y^2 cT) = \dot{m}_a' c_a T_a + \frac{\dot{m}_a'}{r}\beta Q \qquad (3.3)$$

Rate of increase of enthalpy flux over dz

Enthalpy inflow from entrained air

heat generated by a fraction of the entrained air burning with vapor

where β is the fraction of the entrained air that burns with fuel vapor and r is the stoichiometric air fuel mass ratio. The lower heat of combustion Q is the heat generated by the stoichiometric combustion of a unit mass of fuel.

The energy equation can be simplified using the perfect gas equation:

$$\frac{\rho T}{\mu} = \frac{\rho_a T_a}{\mu_a} \qquad (3.4)$$

and the assumption that the molar specific heats are the same for all species. Using in addition Equation 3.1 it can be shown that the energy equation reduces to either of these two forms shown below:

$$\frac{d}{dz}(u y^2) = \frac{2\alpha}{\omega}\left(\frac{\rho}{\rho_a}\right)^{1/2} u y \qquad (3.5a)$$

$$\rho u y^2 = \rho_o u_o y_o^2 + \rho_a \omega [u y^2 - u_o y_o^2] \qquad (3.5b)$$

where

$$\omega = \frac{1}{\left[1 + \frac{\beta Q}{c_a T_a r}\right]} \quad = \text{inverse volume expansion ratio} \qquad (3.6)$$

and the subscript o represents the conditions at the pool surface.

We now define the following parameters, non-dimensional variables, and other non-dimensional parameters.

$u_{ch} = \sqrt{gy_o}$ = characteristic flow velocity (3.7a)

$F = \frac{u_o}{u_{ch}}$ = Froude number at the base (3.7b)

$\xi = \frac{z}{y_o}$ = non-dimensional vertical coordinate (3.8a)

$\eta = \frac{y}{y_o}$ = non-dimensional fire radius at any height (3.8b)

$\sigma = \frac{\rho}{\rho_a}$ = ratio of gas density at any height to the air density (3.8c)

$v = \frac{u}{u_{ch}}$ = dimensionless velocity (3.8d)

$V = v\eta^2$ = dimensionless volume flux (3.9a)

$M = \sigma v^2 \eta^2$ = dimensionless momentum flux (3.9b)

We note; at $\xi = 0$, i.e., at the base of the fire:

$$V = V_o = v_o = F \tag{3.10}$$

and

$$M = M_o = \sigma_o v_o^2 = \sigma_o F^2 \tag{3.11}$$

We now write Equations 3.5a, 3.2 and 3.5b in dimensionless form. Using the above parameters and substituting:

$$\eta^2 = \frac{\sigma V^2}{M} \tag{3.12}$$

we get

$$\frac{dV}{d\xi} = \frac{2\alpha}{\omega} M^{1/2} \tag{3.13}$$

$$\frac{dM}{d\xi} = \sigma(1-\sigma)\frac{V^2}{M} \tag{3.14}$$

and

$$\sigma = \frac{(\sigma_0 - \omega)}{\left(\frac{V}{F}\right)} + \omega \qquad (3.15)$$

3.3.1 Solution of Equations

Equations 3.13, 3.14, and 3.15 constitute a set of three equations in three unknown, namely, V, M, and σ. They can be solved in principle with the initial conditions specified in Equations 3.10 and 3.11. This solution procedure is illustrated below.

Dividing Equation 3.14 by 3.15 and rearranging we get:

$$\frac{dM}{dV} = \frac{\omega}{2\alpha} \frac{V^2}{M^{3/2}} \sigma (1-\sigma) \qquad (3.16)$$

in which σ can be substituted in terms of V from Equation 3.15. The resulting equation is integrated to yield:

$$\left[\left(\frac{M}{M_0}\right)^{5/2} - 1\right] = \frac{5\omega}{4\alpha \sigma_0^{5/2} F^2} \left[\frac{\omega(1-\omega)}{3}\left\{\left(\frac{V}{F}\right)^3 - 1\right\} + \frac{(\sigma_0-\omega)(1-2\omega)}{2}\left\{\left(\frac{V}{F}\right)^2 - 1\right\} - (\sigma_0-\omega)^2\left\{\frac{V}{F} - 1\right\}\right] \qquad (3.17)$$

The above equation gives the relationship between momentum flux and volume flux at any section. All other parameters can be related (as shown below) to the volume flux V and, therefore, it will be treated as the independent variable.

The height above the pool is obtained by integrating Equation 3.13, i.e.,

$$\xi = \frac{\omega}{2\alpha} \int_{V=F}^{V} \frac{dV}{\sqrt{M}} \qquad (3.18)$$

where M is substituted by V from Equation 3.17. Also, for any given value of V:

- σ can be evaluated from Equation 3.15.
- η can be obtained from Equation 3.12 knowning M from Equation 3.17.
- v can be evaluated from the equation:

$$\nu = \frac{M}{\sigma V} = \frac{V}{\eta^2} \tag{3.19}$$

Once σ is known the temperature T at any section can be evaluated by:

$$\frac{T}{T_a} = \frac{\rho_a}{\rho} = \frac{1}{\sigma} \tag{3.20}$$

3.3.2 Certain Simplifications

In general the volume flow at sections above a height of about 1/10 pool radius, will be considerably larger than the gas volume flow at the pool surface. That is, in general:

$$\frac{V}{F} >> 1 \quad \text{and} \quad M >> M_o \tag{3.21}$$

If this condition is assumed, Equation 3.17 can be reduced to:

$$\frac{M}{M_o} \simeq \left[\frac{5\omega^2(1-\omega)}{12\alpha\sigma_o^{5/2}} \frac{1}{F^2}\right]^{\frac{2}{5}} \left[\frac{V}{F}\right]^{\frac{6}{5}} \tag{3.22}$$

Substituting the above in Equation 3.18 and integrating:

$$\xi \simeq 1.49 \left[\frac{F^2\omega^3}{\alpha^4(1-\omega)}\right]^{\frac{1}{5}} \left[\left(\frac{V}{F}\right)^{2/5} - 1\right] \tag{3.23}$$

Substituting in Equation 3.12 for M from Equation 3.22 and for σ from Equation 3.15 we have, after simplifications:

$$\eta^2 \simeq \left[\frac{12\alpha\sigma_o^{5/2}F^2}{5\omega^2(1-\omega)}\right]^{2/5} \left(\frac{V}{F}\right)^{\frac{4}{5}} \left[\frac{\omega}{\sigma_o} + \frac{(1-\frac{\omega}{\sigma_o})}{(V/F)}\right] \tag{3.24}$$

From the above equation it can be shown that the minimum η occurs when:

$$\left[\frac{V}{F}\right]_{\text{MINIMUM } \eta} = \frac{1}{4}\left[\frac{\sigma_o}{\omega} - 1\right] \tag{3.25}$$

Substituting the above in Equation 3.24, it can be shown that the value of minimum radius is:

$$\eta_{MINIMUM} \doteq 1.53 \left[\frac{\omega^{\frac{1}{2}} F^2 \alpha}{(1-\omega)}\right]^{1/5} \left[\frac{\sigma_o}{\omega} - 1\right]^{2/5} \quad (3.26)$$

The height (ξ) at which minimum value of η occurs is obtained by substituting Equation 3.25 in Equation 3.23.

The algorithm for calculating all of the quantities is as follows:

Step #	Parameter(s) Calculated	Equation(s)
1	Calculate the three fundamental parameters of the problem, namely,	
	F	3.7b
	σ_o	3.8c
	α, β are given	
	ω	3.6
2	Choose a value of ξ	
3	(V/F)	3.23
4	η	3.24
5	σ	3.15
6	v	3.19
7	(T/T_a)	3.20

3.4 SPECIFIC EXAMPLE

To illustrate the methodology of calculating the various quantities in the fire, a specific numerical example is worked out below. The values of the physical dimensions and the fuel used are assumed to be the same as the ones used in one of the recent NASA JP-4 fuel fire tests:

	Value	Units
Test Conditions		
Nominal diameter of the pool ($2y_o$)	15.24	m
Quantity of JP-4 fuel burned	6.06	m^3
Duration of burning	380	s
Maximum (estimated) visible fire height	45.7	m
JP-4 Properties		
Density of liquid (at 15 °C)	770	kg/m^3
Heat of combustion (lower) (Q)	4.65×10^7	J/kg
Heat of vaporization	3.3×10^5	J/kg
Flash temperature	340	K
Boiling temperature	520	K
Density of vapor at boiling temperature	1.8	kg/m^3
Liquid regression rate	10^{-4}	m/s
Specific heat of air at constant pressure	10^3	J/kg K
Air fuel mass ratio (r)	17	
Air temperature (T_a)	290	K
Density of air (ρ_a)	1.2	kg/m^3

Calculations of Parmaeters

Parameter	Symbol	Equation	Value	Units
Characteristic Velocity	u_{ch}	(3.7a)	8.64	m/s
Vapor velocity at the liquid surface	u_o	$\frac{10^{-4} \times 770}{1.8}$	$= 4.28 \times 10^{-2}$	m/s
Froude number	F	(3.7b)	4.95×10^{-3}	
Entrainment coefficient	α	(assumed)	0.1	
Mixedness parameter	β	(assumed)	1.0	
Dimensionless base density	σ_o	(3.8c)	1.5	
Inverse volumetric expansion ratio	ω	(3.6)	0.0988	

When the density of vapor at the base is higher than that of the air density and the vapors are released at very low velocity, the momentum Equation 3.2 shows that the net momentum will start to decrease. However, in a real fire, because of the inflow of air close to the ground (generated by the buoyancy in the upper parts of the flame), and its turning at the flame surface, an upward shear is induced on the heavy vapors at the liquid pool surface. This phenomenon is not considered in our simple model. However, its effect can be incorporated very simply (note, however, this is artificial) by assuming that the effective density of vapor at the base of the flame is equal to that of air.

Therefore, we consider $\sigma_o = 1$.

Solution

The solutions obtained from the complete set of equations 3.17, 3.18, 3.15, 3.12, and 3.19 for the parameters M, ξ, σ, η, and v respectively are shown in Figure 3.3 plotted as functions of (V/F). In Figure 3.4 the same results are plotted as functions of the height coordinate ξ. Also plotted in this figure is the temperature within the fire as a function of the height. In Figure 3.5 the same dependent variables have been plotted but with the assumption that there is no complete combustion of the entrained air (i.e., $\beta = 0.7$). To obtain the results shown in Figure 3.5, the simplified formulae 3.22, 3.23, 3.24, etc., were used.

Results and Discussion

The results show clearly necking of the fire. Also, the predicted minimum radius (Equation 3.26) using the simple model agrees very closely with the actually observed data (discussed in the next chapter). The velocity predicted by the model at the location of the anemometer (5.58 m above pool) is also very close to the measured velocity. The temperature at the same location is high if the mixedness parameter (β) is assumed to be 1. However, if the mixedness parameter value is 0.7, then the predicted temperature and the measured temperature agree reasonably well.

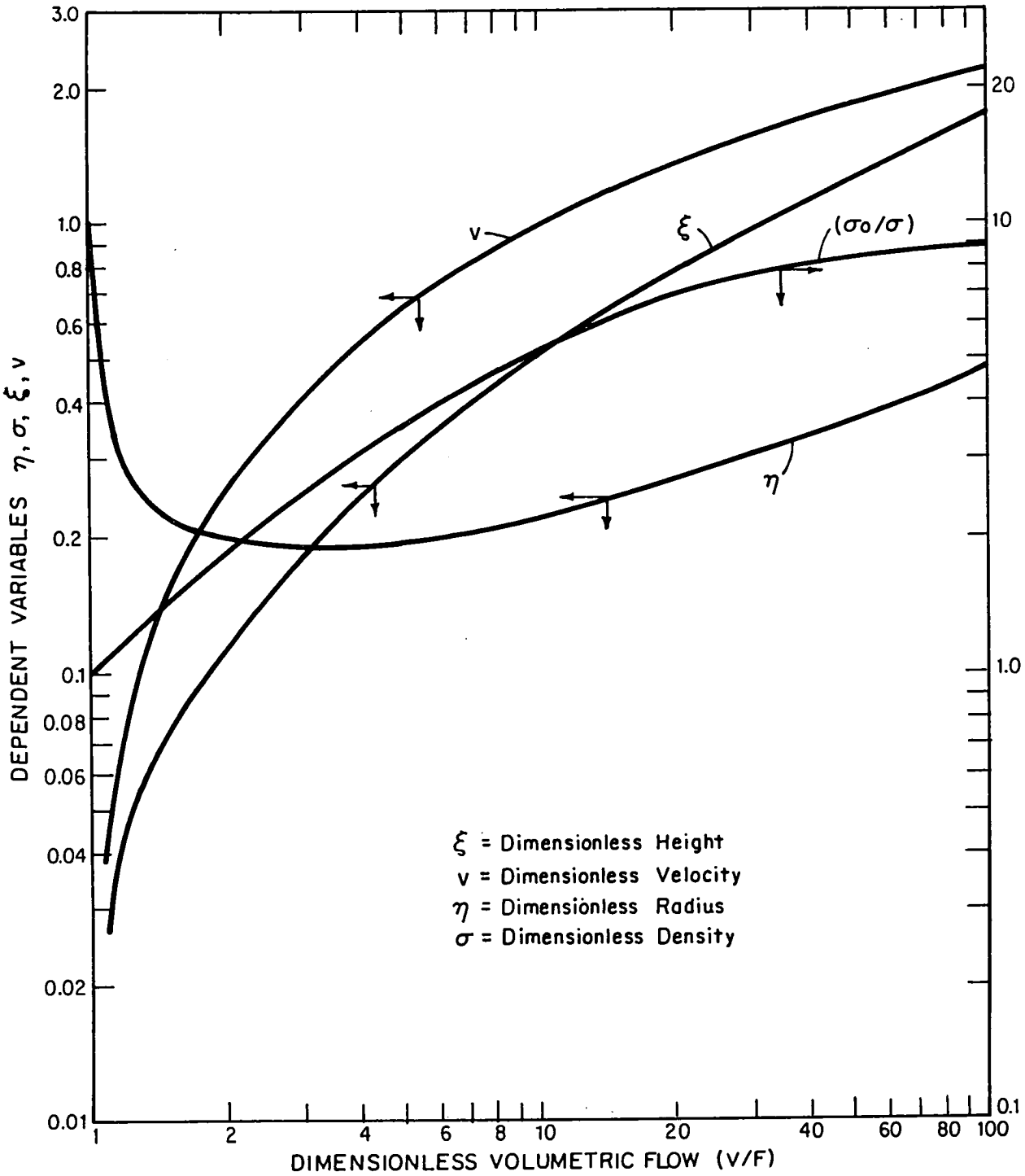

FIGURE 3.3. VARIATION OF DIMENSIONLESS RADIUS, GAS DENSITY, HEIGHT WITHIN THE FIRE AND VELOCITY WITH DIMENSIONLESS VOLUMETRIC FLOW

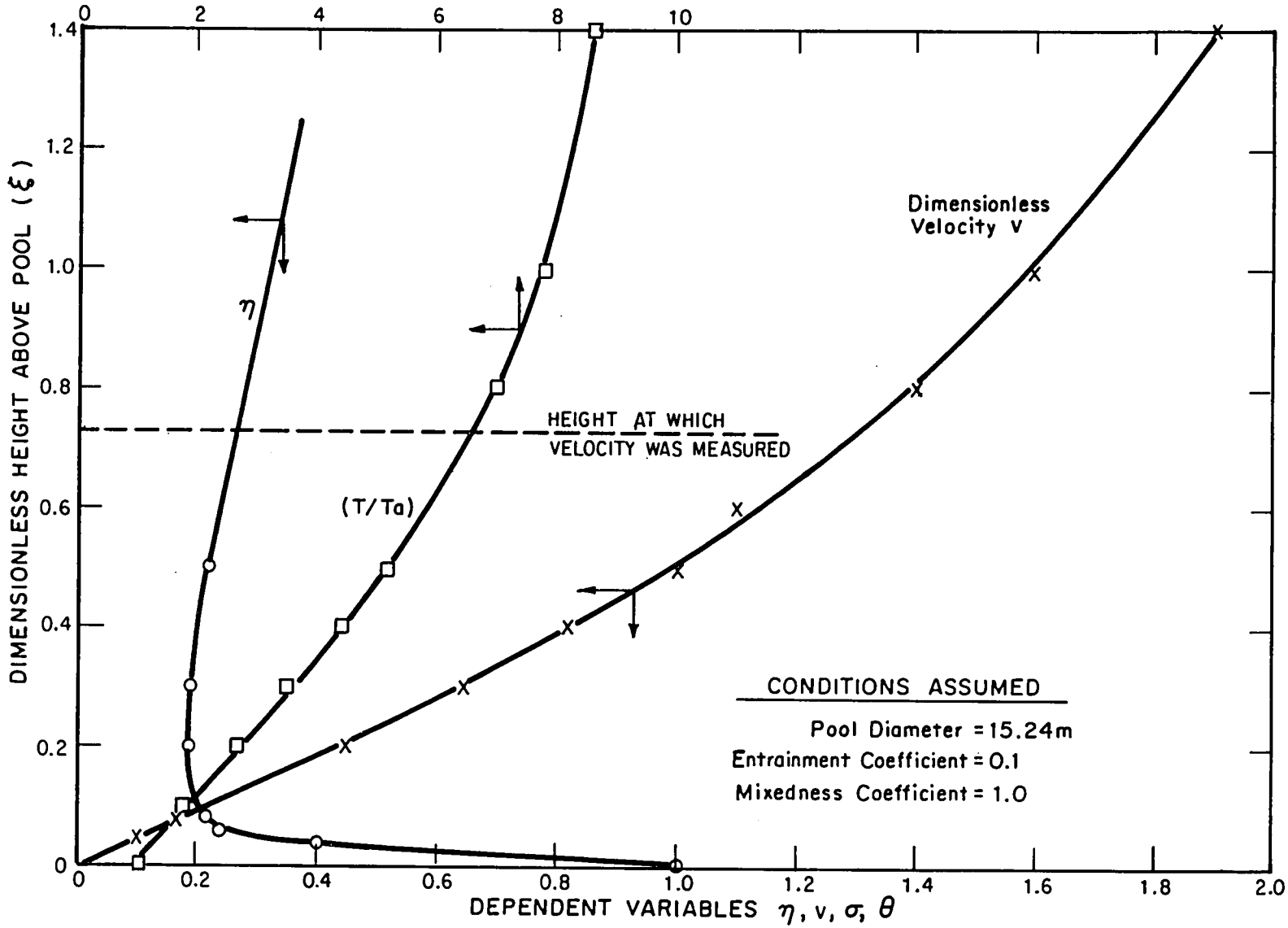

FIGURE 3.4. VARIATION OF DIMENSIONLESS VARIABLES WITH THE HEIGHT WITHIN THE FIRE

The principal advantage of the model presented is its simplicity and the ease with which the variations of different parameters within the fire can be predicted, using a simple pocket calculator. The limitations of the model are that it (i) is a steady-state model, (ii) does not take into account details of turbulent mixing, (iii) does not give the radial distribution of the properties accurately, and (iv) does not treat the combustion chemistry at all. However, in spite of these limitations, the model predicts the centerline parameters to within sufficient accuracy for engineering purposes.

It is noted that the model discussed above is applicable only as long as there is fuel vapor remaining in the plume to burn. That is, the calculations can be extended up to the height at which the total mass of air "burned" is equal to the stoichiometric mass required to combust with the fuel. It can be shown that:

$$\frac{\text{Ratio of mass flow rate of gases at stoichiometric height}}{\text{mass flow rate at the pool surface}} = \left(1 + \frac{r}{\beta}\right) \quad (3.27)$$

$$\therefore \quad \left(\frac{\sigma}{\sigma_0}\right)_s \left(\frac{V}{F}\right)_s = \left[1 + \frac{r}{\beta}\right] \quad (3.28)$$

By using the Equation 3.15 it can be shown easily that the above equation reduces to:

$$\left(\frac{V}{F}\right)_s = \left[1 + \frac{\sigma_0 r}{\beta \omega}\right] \quad (3.29)$$

where the subscript s denotes stoichiometric value. Substituting Equation 3.28 in 3.23 results in the estimate for the stoichiometric height.

It is assumed in this model (a la Steward, 1972), that above the stoichiometric height there is no combustion and, therefore, the ordinary plume equations apply. The region above $\xi = \xi_s$ can be analyzed by putting $\omega = 1$ in the equations and assuming the initial conditions to be the conditions at the stoichiometric height.

4. COMPARISON OF MODEL PREDICTIONS WITH EXPERIMENTAL DATA

In this chapter the fire centerline temperature data, the velocity data measured at one location within the fire and the observed fire diameter with height are compared with the predictions for the same parameters using the model developed in Chapter 3. Because of the assumptions made in the model with regard to the uniform profiles (tophat profile) of temperature and velocity it is not possible to compare measured radial variations with model predictions. Also, no chemistry data can be compared because the model assumes instantaneous mixing of air and its partial reaction with fuel vapors. The comparison in this chapter should therefore be construed as fine tuning of the model by determining the free parameters using the experimental data.

4.1 TEMPERATURE DATA

Figure 4.1 shows the experimentally measured temperature data along the vertical centerline from two fires of 15.7m diameter. The range of fluctuations in the measurement is also indicated. It is seen that the centerline temperature increases rather rapidly from about 900 K very close to the pool surface* to about 1100 K by about 3m height. Above this height the temperature increase is moderate and the temperature is substantially constant (1400 - 1500 K) from 6m height to 24m.

The predicted variations in temperature along the centerline of the fire are also shown in Figure 4.1. The parameters varied in the model are the temperature of the fuel vapor as it is released from the boiling pool, the air entrainment coefficient (α), and the mixedness factor (β). Lines 1 and 2 indicated are drawn for an initial vapor temperature of 300 K, line #3 is for 500 K and line #4 is for 900 K. The values of α and β used are shown in the figure.

It is seen from Figure 4.1 that the model predicts the qualitative behavior of the experimentally observed temperature variation

---

*It is doubtful if this temperature recorded very close to the pool surface is indeed the local gas temperature. The thermocouple may be recording its own radiative equilibrium temperature since it was not radiation shielded. The actual gas temperature is expected to be about 500 K.

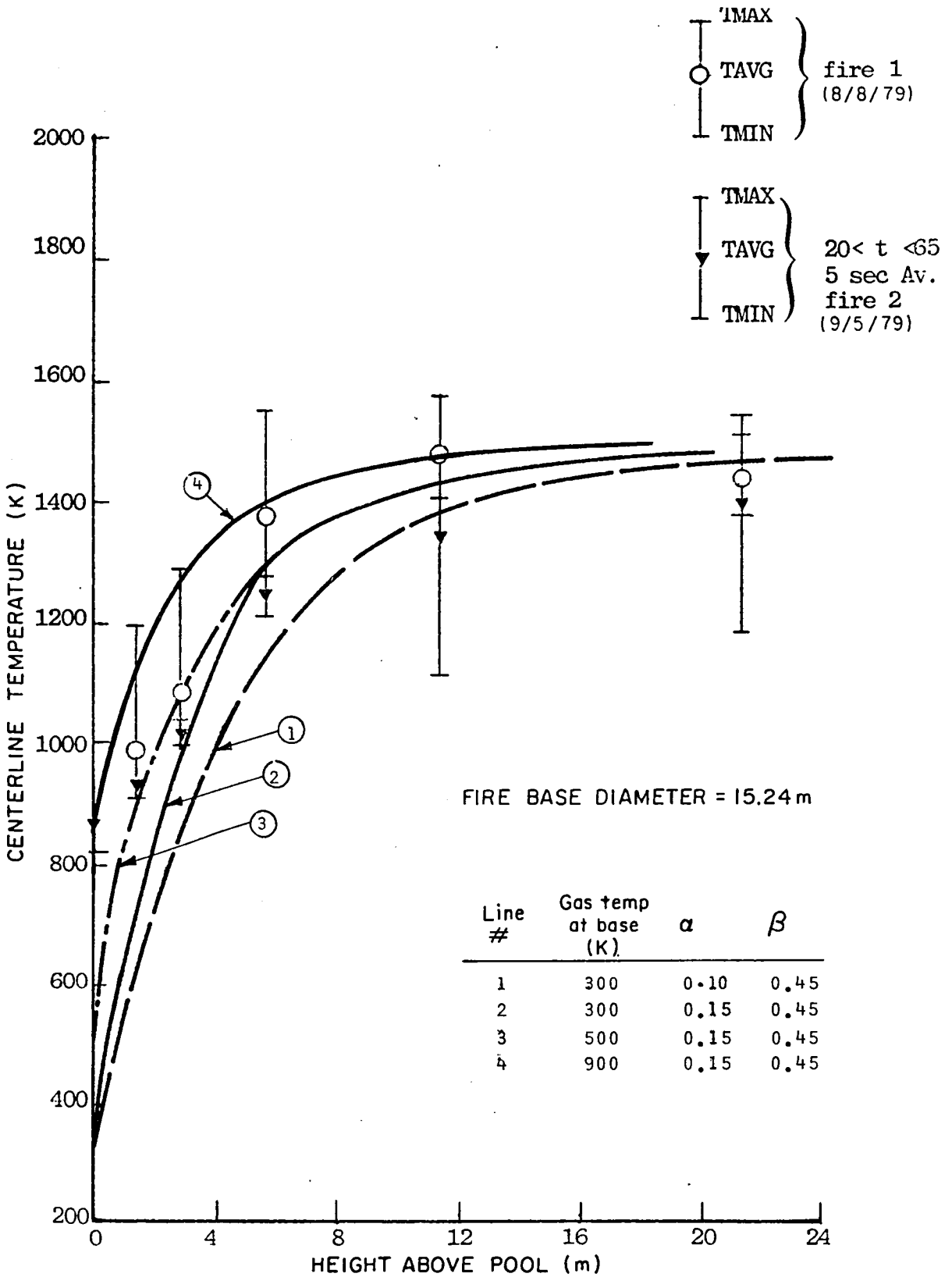

FIGURE 4.1. COMPARISON OF EXPERIMENTAL CENTERLINE TEMPERATURE DATA AND MODEL PREDICTIONS

extremely well. In order to make the prediction and data agree reasonably well quantitatively, the values of the parameters in the model have to be adjusted. It is also seen that the correct initial condition input to the model is essential if the temperature data and the predictions for heights lower than 4m are to agree.

A change in the value of any of the important parameters affects the predicted temperature in different ways. An increase in the base vapor temperature increases the predicted temperature with height at all heights. However, the maximum temperature predicted within the fire remains unaffected. Similarly an increase in the value of the entrainment coefficient (α) raises the predicted temperature value at every given height and at the same time not affecting the final temperature. The higher the value of α the lower the height at which the peak temperature is reached. Variation in the value of the mixedness coefficient (β) affects the peak temperature vs height curve. For example, if β is assumed to be unity (i.e., all of the entrained air burns immediately) then the temperature continuously rises with height (without ever showing an asymptotic behavior) up to the stoichiometric height. Concurrence of experimental data and the model predictions therefore can be achieved only if the non-uniform mixing of air is assumed. Figure 4.1 shows that reasonable agreement between the data and the model predictions occur for values of $\alpha = 0.15$ and $\beta = 0.45$. Table 4.1 shows the calculated values of fire radius, temperature and gas velocity at a height of 5.73m and also the maximum temperature in the fire for different values of α and β.

It is recalled that the model assumes no property difference between fuel vapor, burnt gas and air, because of the requirements of constant specific heats and perfect gas behavior. The agreement between data and model observed implies that this assumption is justifiable in most situations except perhaps at the very low heights. Secondly we also note the insensitivity of the predictions to slight changes in the value of the entrainment coefficient. However, small changes in the value of mixedness factor (β) results in large variations in the peak temperature prediction. The value of β that best fits the

TABLE 4.1

PREDICTED FIRE RADIUS, VELOCITY, TEMPERATURE AT 5.73m HEIGHT AND MAXIMUM TEMPERATURE WITH VARIATION IN α AND β VALUES[†]

Entrainment Coefficient (α)	Mixedness Coefficient (β)	Radius of Fire (m)	Velocity at 5.73m Height (m/s)	Temperature at 5.73m Height (K)	Maximum Temperature (K)
0.1	0.45	2.2	9.4	1180	1520
0.15	0.45	2.7	9.6	1290	1520
0.2	0.45	3.3	9.7	1353	1520
0.3	0.45	4.4	9.7	1420	1520
0.15	0.50	2.8	10.0	1400	1655
0.20	0.50	3.4	10.1	1472	1655

[†]Assumed vapor temperature at the pool surface = 500 K (therefore $\sigma_o = 0.58$)

Ambient air temperature = 288 K

model predictions with experimental data is 0.45. The meaning of this result is somewhat difficult to interpret. One interpretation, assuming that the model correctly represents what is happening inside the fire, is that only about 45% of the mass of air entrained at any section burns immediately. The other interpretation is that the diffusion of air entrained at any section is slow so that the mixing efficiency is 45%. In effect this value of 0.45 for β is the resultant of averaging out of the effects of many of the competing processes.

Recently, a detailed turbulent fire model has been developed by Science Applications, Inc. (SAI). This model has been reported in a preliminary report (Harsha et al., 1979). Figure 4.2 shows the experimental centerline temperature data and the predictions obtained from the SAI model. The SAI model predictions seem to be in variance with the experimental data. It is our understanding that the model is being further revised and improved. As such the model predictions are to be assumed as preliminary.

4.2 VELOCITY DATA

The vertical centerline velocity was measured in two experiments (only) at a height of 5.73m above the pool. These data are shown in Figure 4.3. Also shown in Figure 4.3 are the theoretical predictions for the variation of vertical velocity with height for three different initial temperature values. The entrainment coefficient and the value (α) of the mixedness factor (β) were respectively 0.15 and 0.45. Perturbations of the values of α over a small range indicated that velocity profiles were insensitive and that the important parameters were the base temperature of the fuel vapor and the mixedness factor β.

A comparison of the predictions and experimental data indicates that the use of fuel boiling temperature for the vapor temperature under-predicts the velocity at 5.7m height, whereas the use of 900 K base temperature seems to give proper values for the velocity. It is recalled that the accuracy of 900 K temperature, which was indeed measured close to the pool surface, was questioned earlier. The velocity data seem to further corroborate the thermocouple reading. However, if the temperature data at the base of the fire is open to question, the model will predict measured velocity values only if a variable mixedness factor with height is assumed. That is, in effect

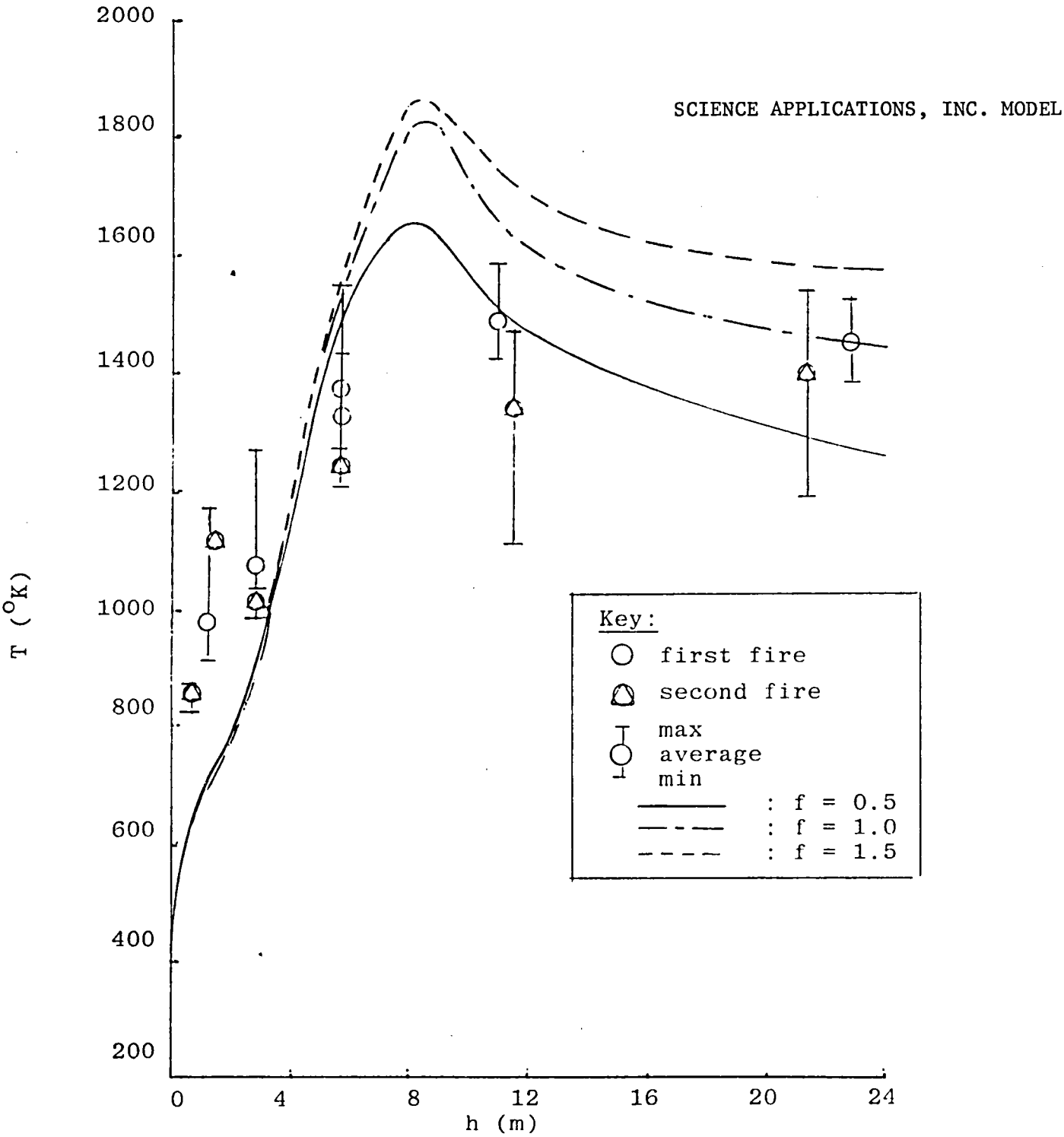

FIGURE 4.2: COMPARISON OF COMPUTATIONS INCORPORATING FLUCTUATING CHEMISTRY MODEL WITH CENTERLINE TEMPERATURE DATA*

*Obtained by Science Applications, Inc.

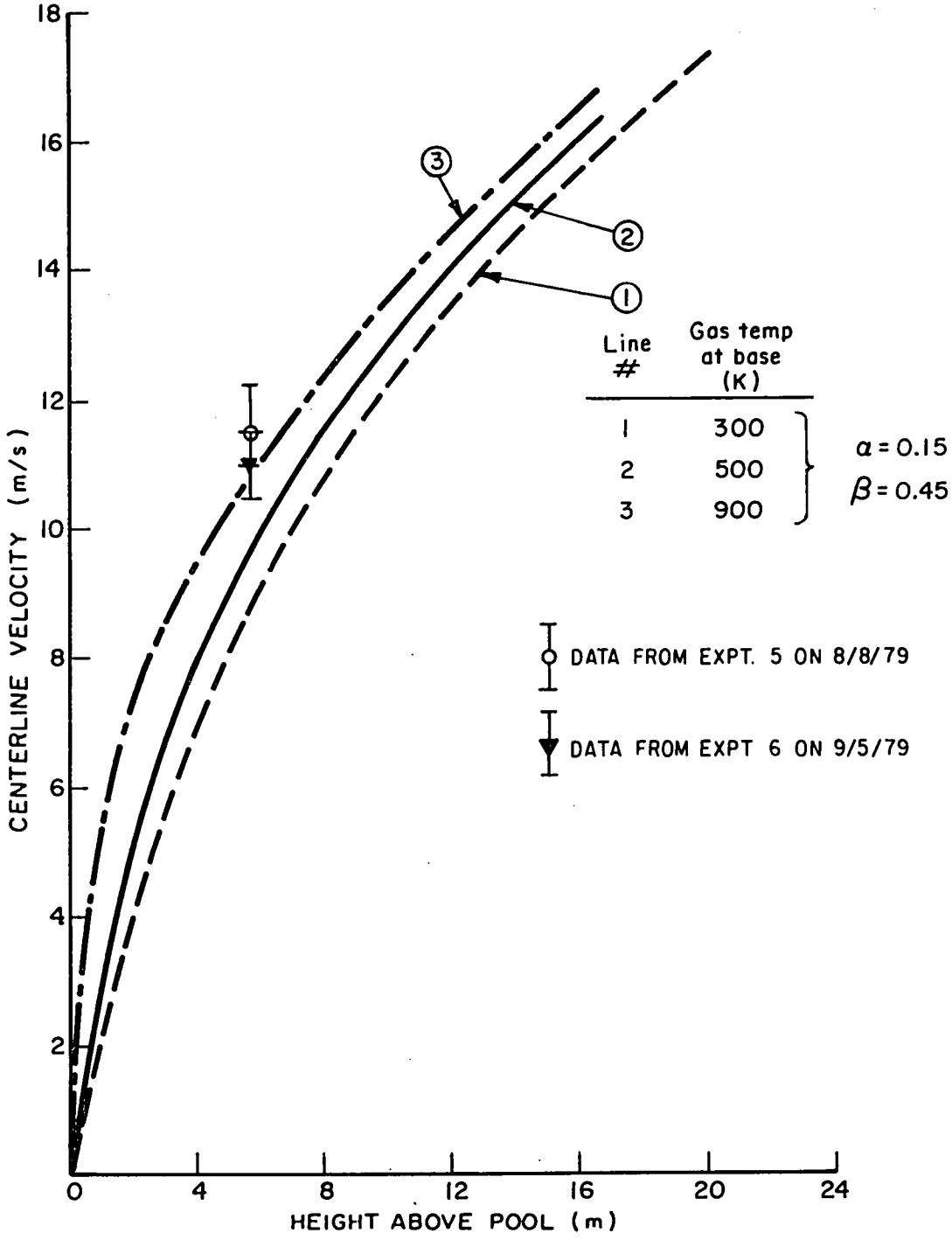

FIGURE 4.3. COMPARISON OF EXPERIMENTAL VELOCITY DATA AND THEORETICAL PREDICTIONS

better mixing of air at the fire base (i.e., higher β values) has to assumed with progressively decreasing mixing efficiency. Whether this model is justifiable is difficult to say; the data available are very limited to corroborate or contradict the variable mixing efficiency (with height) thesis.

4.3 FIRE DIAMETER WITH HEIGHT

Motion picture records of the experiments show two interesting phenomena related to the fire diameter with height. The first phenomenon is one of fire necking; that is the diameter of the fire very rapidly decreases from the pool diameter to a significantly low value within a relatively short distance above the pool (1 to 2 meters). Subsequently the diameter increases with height rather uniformly. The second phenomenon that is observed is the regular pulsative release of blobs of fire from the pool through the entire fire column. In the latter process the dimension of the "neck" of the fire also fluctuates with a period of about 2 seconds.

The theoretical analysis developed in Chapter 3 is based on steady state consideration. Therefore, the comparison between model predictions and the field experimental data on fire diameter may be difficult to make, because of the pulsations mentioned above. A second difficulty is encountered in comparing fire diameters from motion picture films and model predictions. The fire size observed in motion picture records is the soot profile, i.e., the edge of visible soot boundary. The fire radius predicted by the model is a mathematical entity within which all properties are uniform at any given height. However, in spite of these difficulties the shape of the fire radius vs height curves obtained from measurements (time averaged) and model predictions can be compared.

Figure 4.4 shows the predicted fire radius variation with height for different values of the parameters. The curves show the characteristic necking of the fire and its subsequent expansion. Unfortunately, the data on fire diameter variation with height are not available at this time. Therefore the theoretical predictions shown in Figure 4.4 cannot be compared with experimental results.

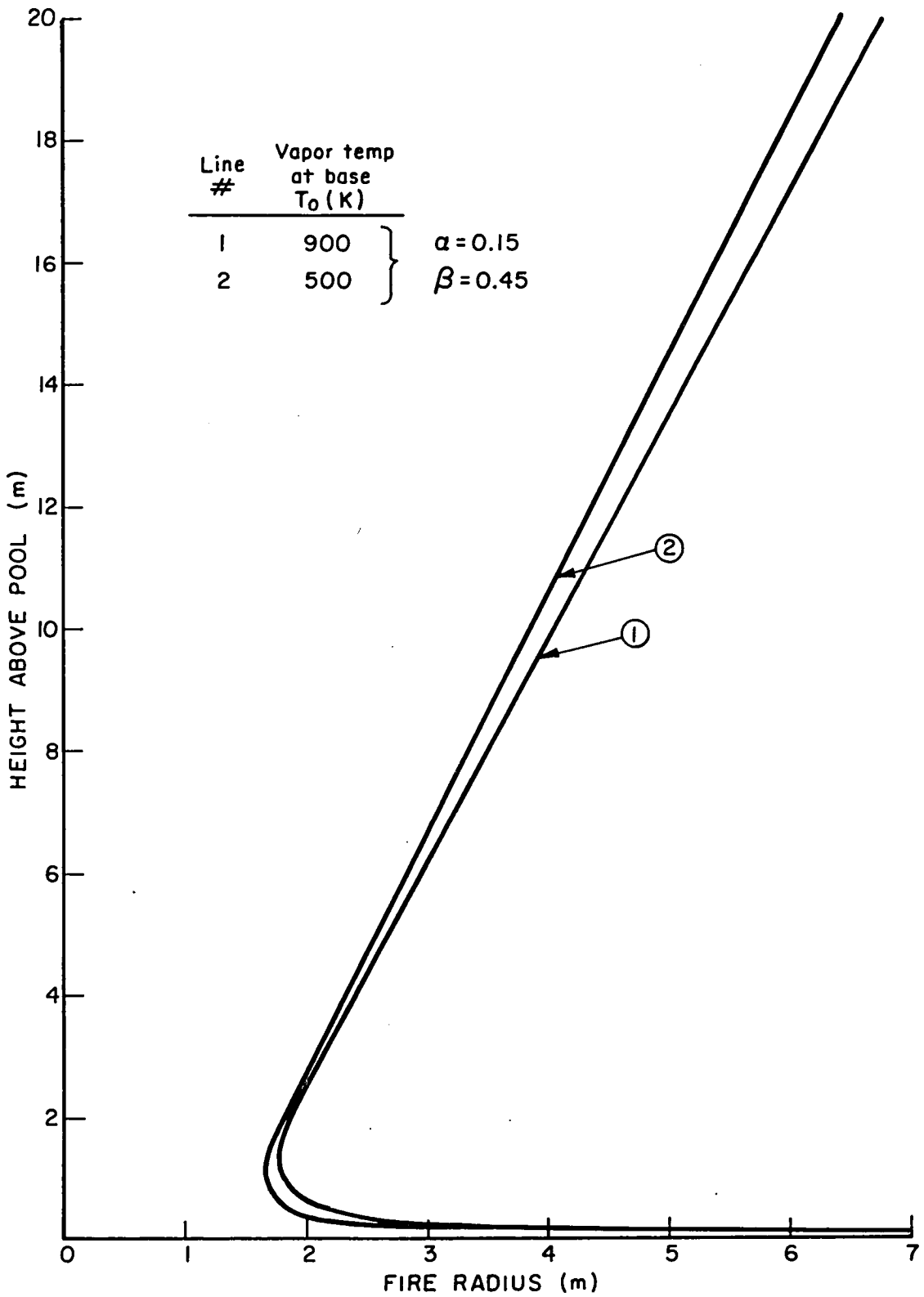

FIGURE 4.4. PREDICTED FIRE RADIUS VARIATION WITH HEIGHT

CONCLUSIONS

- The experimental data and the theoretical prediction agree reasonably well both in the type of behavior of parameters with height as well as quantitative terms.
- Quantitative agreement is obtained between data and predictions when a value of 0.15 is used for the entrainment coefficient and 0.45 for the mixedness factor.
- The model predicts the necking of the fire which was observed in the field tests. Because the data on fire diameter have not been reduced from the movie films of the experiments, it has not been possible to compare the actual and predicted values.
- Because of the top hat profile assumed in the model only mean values of the variables can be predicted. Comparison of model predictions with centerline data (which in many cases may represent peak values at any section) has to be reviewed judiciously.
- Since model is based on overall considerations of energy release in combustion and not on the details of the chemistry of combustion, it is not possible to compare the chemical specie concentration results gathered during the tests with theoretical predictions.

5. REVIEW OF DATA FROM EXPERIMENTS REPORTED IN THE LITERATURE

Experimental data for the temperature, velocity and specie distributions in a turbulent fire are very scarce. They are almost non-existant for field size fires. To the best of our knowledge there are only two sources in the literature in which the data on the distributions of temperature, velocity, etc. in a turbulent fire are discussed. These are reviewed below along with the data from the JP-4 fuel fire tests conducted by NASA.

5.1 EXPERIMENTS AT THE NATIONAL BUREAU OF STANDARDS (NBS)

McCaffrey (1978) has published temperature and velocity measurements gathered in a 0.3m x 0.5m methane (turbulent) flame. Time averaged centerline temperatures and velocities measured are shown in Figures 5.1 and 5.2, respectively for different burning rates. It is noted that unfortunately the plots are not on dimensionless coordinates.

The temperature data obtained from the NASA experiments (two tests each with 15.2m diameter JP-4 fuel pool fires) are also plotted in Figure 5.1. It is seen that the agreement between McCaffrey data and the NASA results are reasonable. A comparison of the results indicates the following:

- The agreement between the results seems to indicate that no matter what the fire size or the type of hydrocarbon fuel burnt is, the peak temperature within a fire is about 1500 K.
- The NASA fire temperature is consistently higher than in the small NBS fires. This may be because in small fires which are not optically thick, the thermocouple at the center of fire may in fact be influenced by radiative losses (hence reading a lower temperature).
- Both McCaffrey data and NASA data indicate that the temperature within the fire reaches a maximum and then remains essentially the same for a significant height through the fire.
- For very large fires the abscissa scale has to be extended in the direction of lower values.

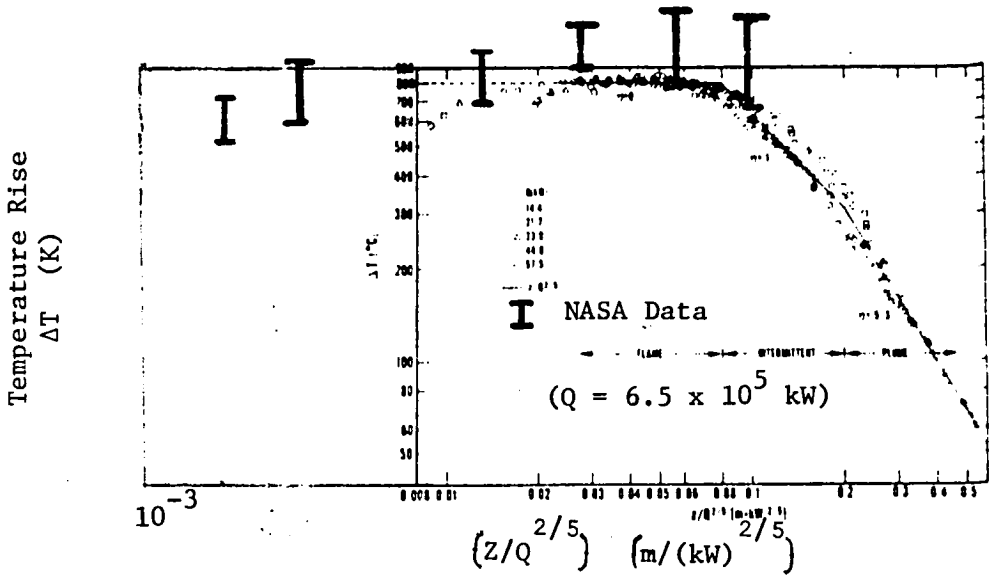

FIGURE 5.1: COMPARISON OF McCAFFREY DATA AND NASA RESULTS FOR CENTERLINE FLAME TEMPERATURE

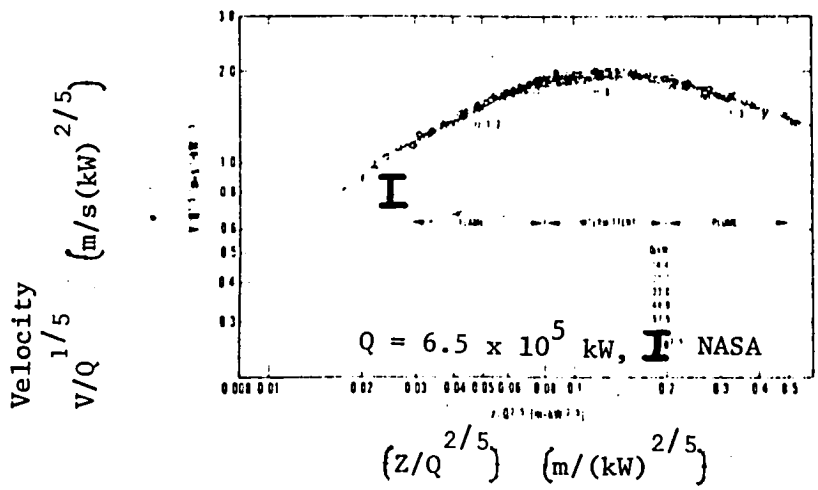

FIGURE 5.2: COMPARISON OF McCAFFREY DATA AND NASA RESULTS FOR CENTERLINE FIRE VELOCITY

In Figure 5.2 the velocity data obtained in the NASA experiments are also indicated. It is seen that the small scale test results and the large scale test data agree quite well indicating that the scaling parameters chosen (on the abscissa and ordinates) are reasonable. However, we do note that the velocity is not a simple function of the height and heat release rate, but depends on other parameters such as the Froude number at the base, type of fuel, entrainment rate, etc. These have all been taken into account in the model developed in Chapter 3.

5.2 MEASUREMENTS OF SPECIE CONCENTRATIONS WITHIN A FIRE

Alger et al. (1979) have reported tests conducted with 3m diameter fires in which temperature and specie concentration data have been measured. Two types of fuels were used, namely, methanol and JP-5 fuel. The specie concentration results for methanol only are published.*

The specie concentration data for oxygen, CO, CO_2 and H_2O (vapor) are plotted as fractions of nitrogen content at several different heights at the centerline of the fire. The results from recent NASA experiments and those data for methanol from Alger's experiments are shown in Figures 5.3 through 5.6. The abscissa of the graphs are mass fractions of species as a function of nitrogen content and the ordinate is the nondimensional height through the center line of the fire.

It is difficult to compare Alger's data with the data from the present experiments because not only are the fire sizes different but the fuels are also different. However, the following qualitative differences can be noticed.

- Smaller size flame seems to be better ventilation, that is, the oxygen content at the center is quite high in the smaller (3m diameter) fire than in the larger JP-4 fire (15m diameter).

---

*Recent telephone discussions with the principal author indicates that data for JP-5 are not easily accessible, since the tests were conducted 4 to 5 years ago.

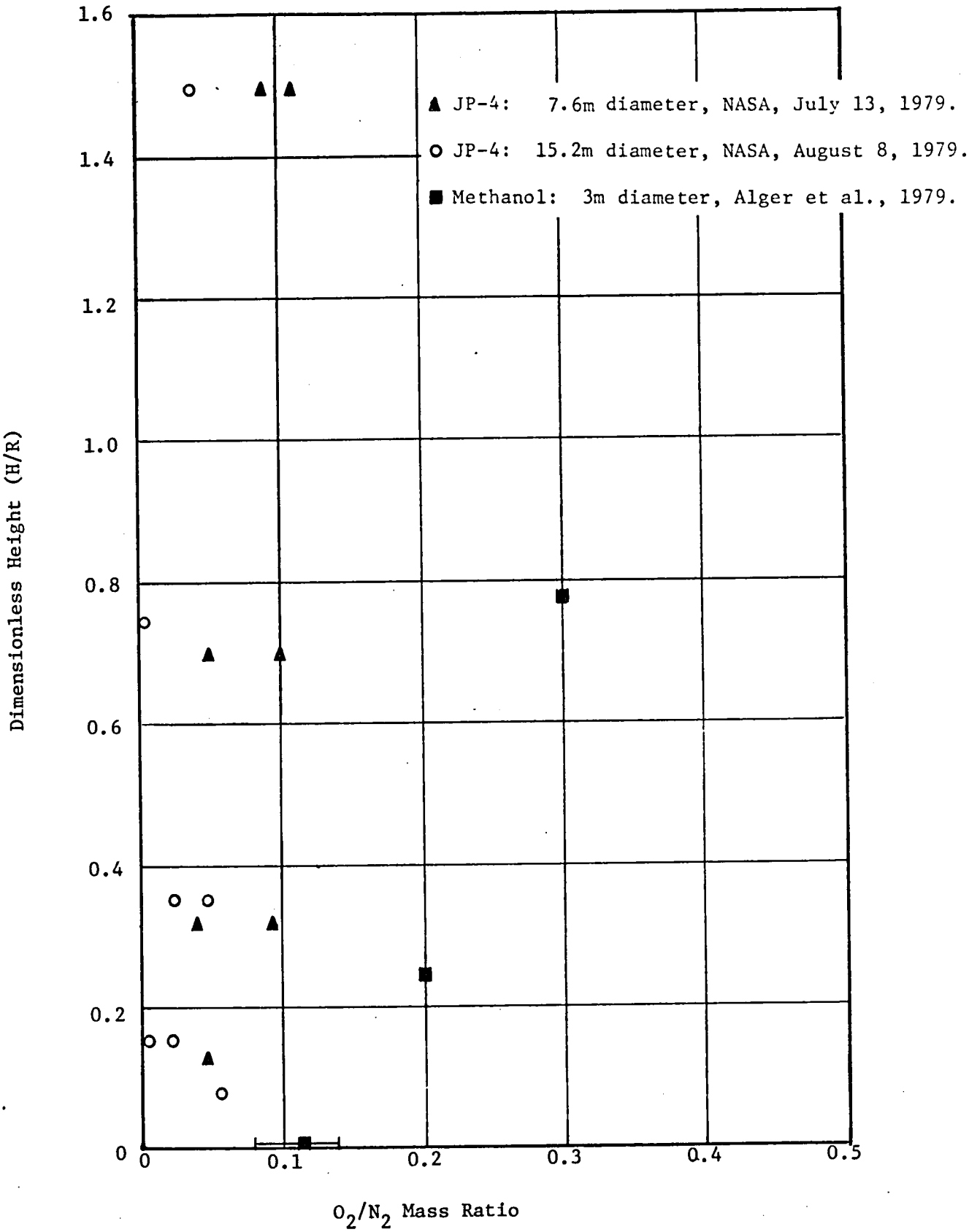

FIGURE 5.3: VARIATION OF CENTERLINE OXYGEN TO NITROGEN MASS FRACTION WITH HEIGHT

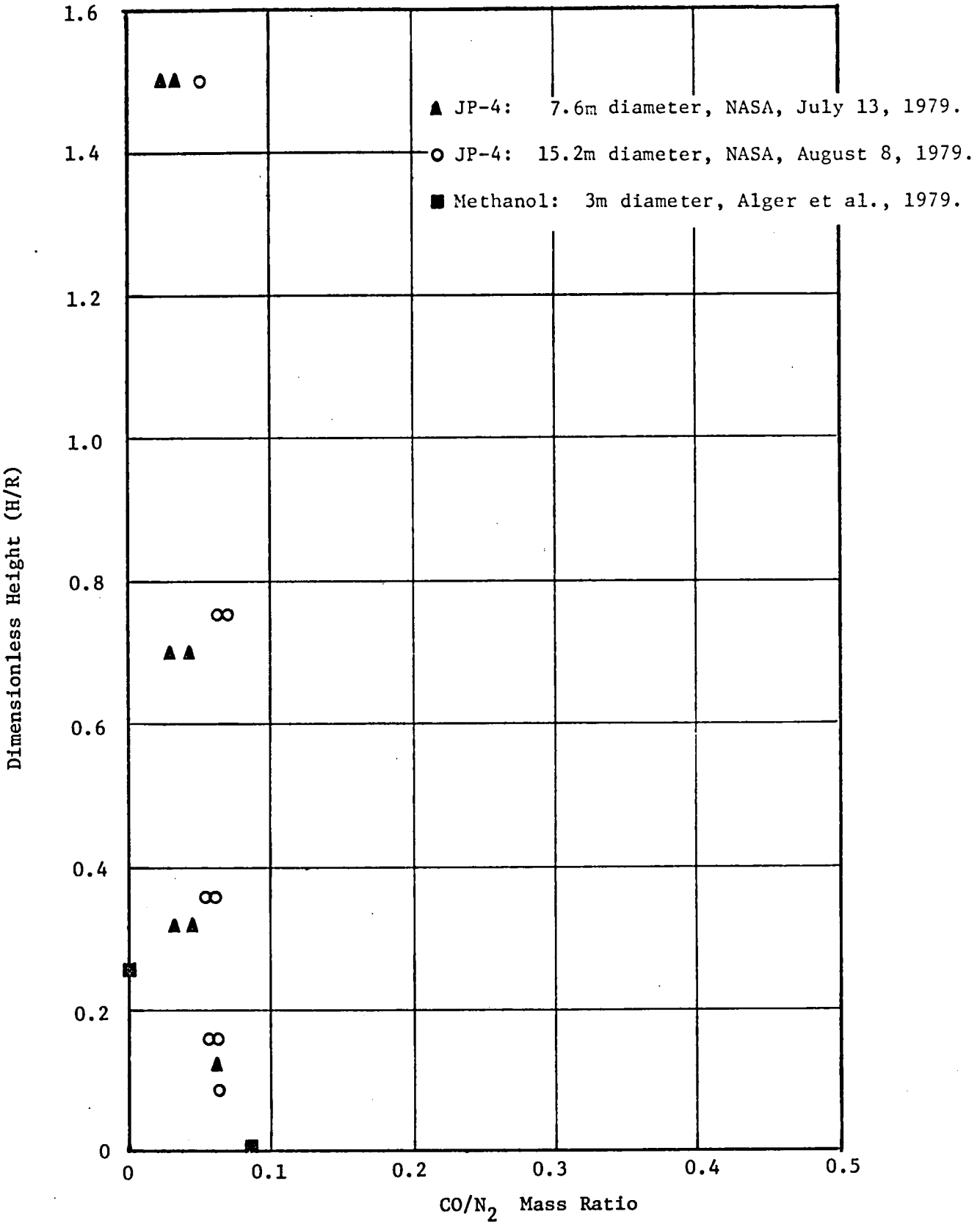

FIGURE 5.4: VARIATION OF CENTERLINE CARBON MONOXIDE TO NITROGEN MASS FRACTION WITH HEIGHT

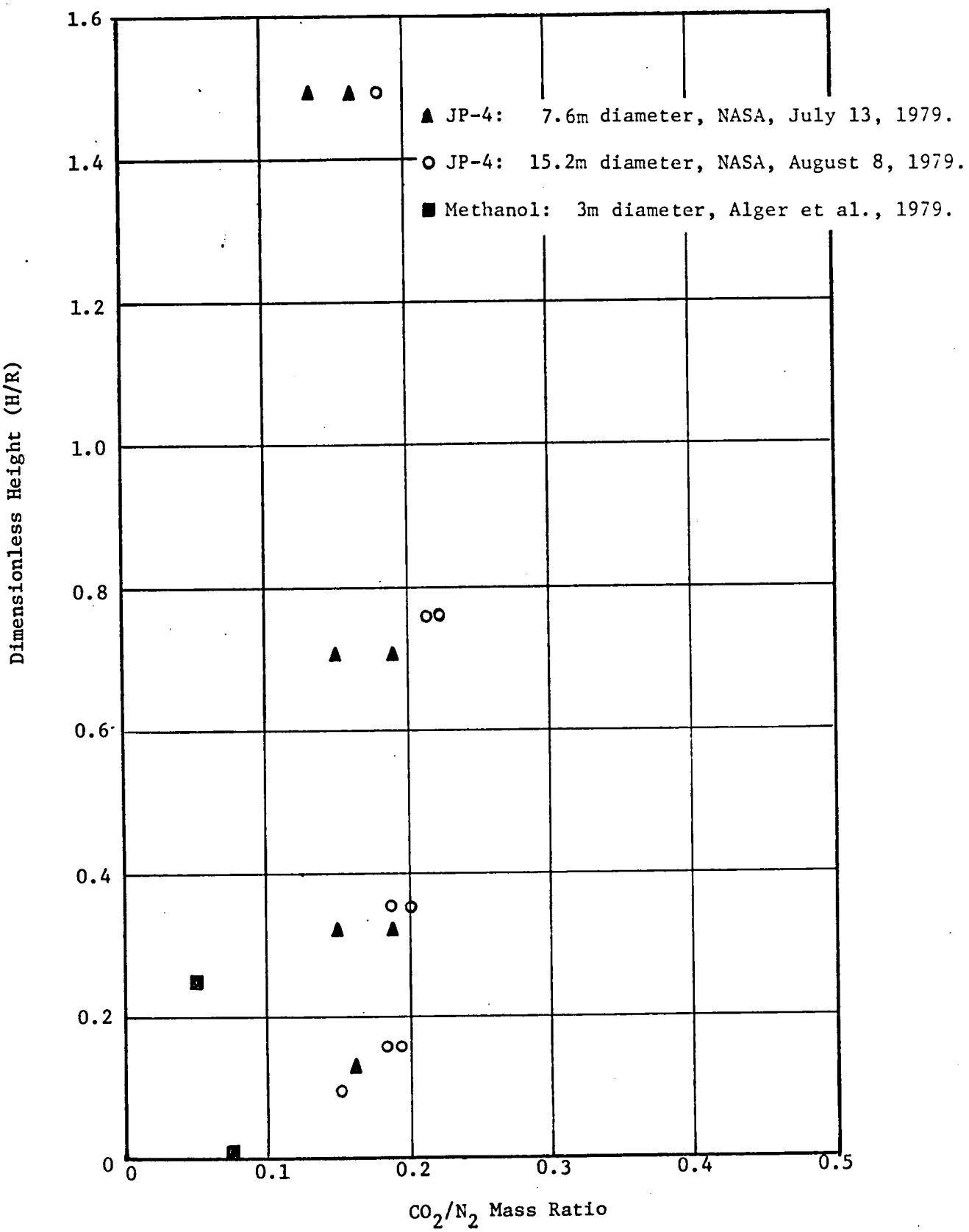

FIGURE 5.5: VARIATION OF CENTERLINE CARBON DIOXIDE TO NITROGEN MASS FRACTION WITH HEIGHT

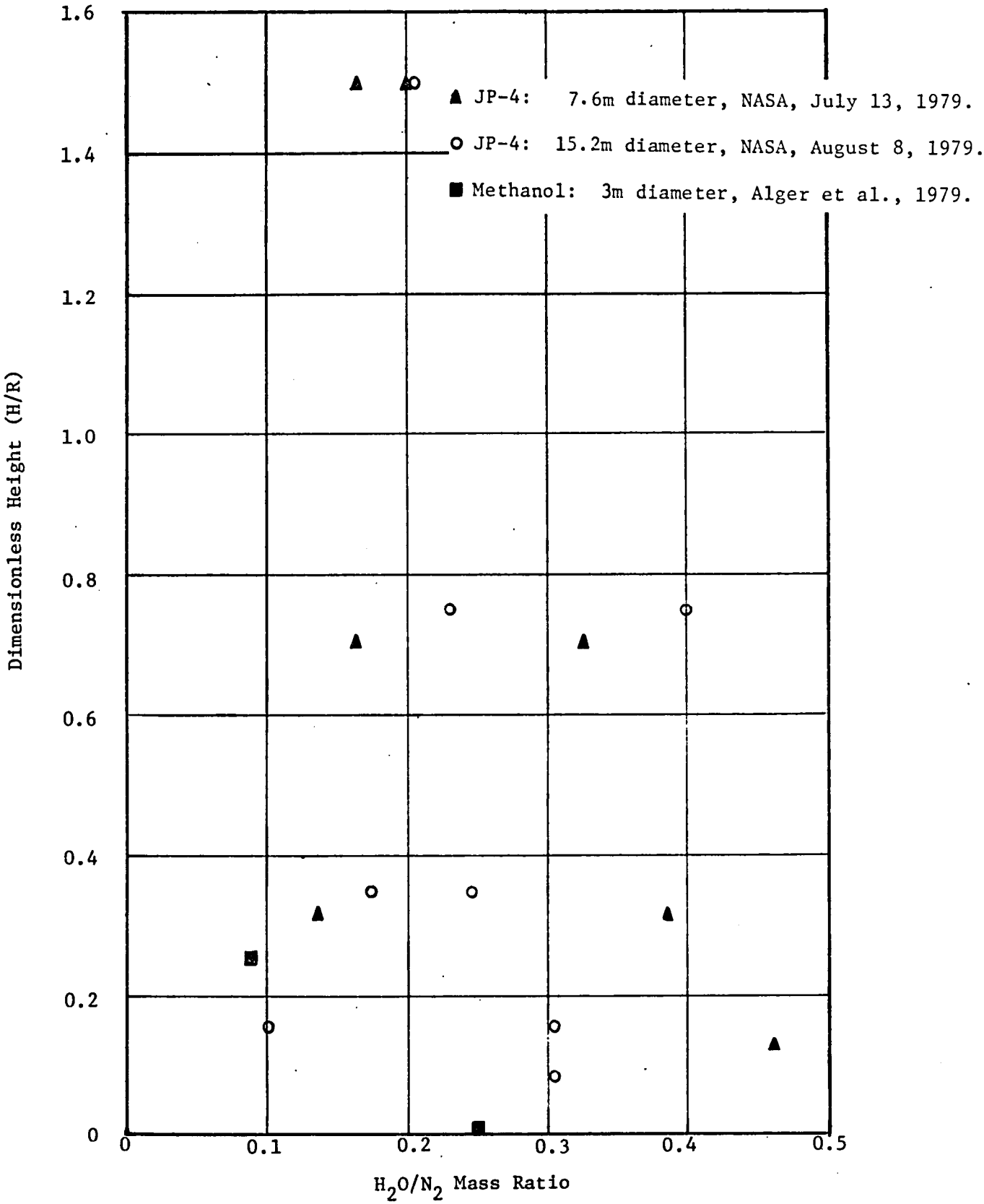

FIGURE 5.6: VARIATION OF CENTERLINE WATER VAPOR TO NITROGEN MASS FRACTION WITH HEIGHT

- In the methanol fire the CO level rapidly decreases in about a height of 0.2 fire radius whereas in the large fire CO is measured up to about 1.4 radius in height. This is additional indication of good combustion at the center of fire for methanol. It could also be interpreted as excess air being present in the center.
- The CO_2 variation with height indicates that in the JP-4 fire the combustion is continuing up to (and perhaps beyond) H/R of 1.5 whereas in the methanol flame most of combustion probably takes place very close to the fuel surface.
- The graph of water vapor distribution is very difficult to interpret. There is little reproducibility in the data. The noisiness in the data can be attributed to the difficulties in measuring water vapor content. Any small liquid condensation in the measuring instrument leads to significant errors in the estimate of water vapor content.

The overall conclusion from the data presented is that in the JP-4 fuel fire there is very little oxygen at the center of the fire up to a height of 1.5 fire radius. That is, combustion is still taking place. Also the near constant mass ratios of O_2, CO and CO_2 with height indicates that a constant fraction of the entrained air is participating in combustion.

NOMENCLATURE

Symbol	Definition	Units
C	Specific heats of gases	J/kg K
D	Diameter of the fire base - pool diameter	m
F	Froude number (Eq. 3.7b)	
g	Acceleration due to gravity	m/s^2
$\dot{m}_a'$	Mass rate of entrainment of air per unit height	kg/m s
M	Dimensionless momentum	
Q	Lower heat of combustion of fuel	J/kg
r	Stoichiometric air fuel mass ratio	
T	Temperature of gas	K
u	Centerline mean upward gas velocity	m/s
u_{ch}	Characteristic velocity (Eq. 3.7a)	m/s
U	Free stream velocity	m/s
v	Dimensionless velocity (Eq. 3.8d)	
V	Dimensionless volumetric flow (Eq. 3.9a)	
y	Radius of fire at any height	m
z	Vertical coordinate	m

Greek Letters

α	Entrainment coefficient
β	Mixedness factor (fractional mass of entrained air that burns immediately with a stoichiometric mass of fuel).

NOMENCLATURE (continued)

Greek Letters	Definition	Units
η	Dimensionless radius (2y/D)	
μ	Molecular weights of species	kg/kmole
ξ	Dimensionless vertical coordinate	kg/m^3
ρ	Density of gases	
σ	Ratio of gas density to that of air	
ω	Inverse volumetric expansion ratio (Eq. 3.6)	

Subscripts	
a	Air
ch	Characteristic value
o	Initial condition - refers to just above pool surface

REFERENCES

Alger, R. S., R. C. Corlett, A. S. Gordon and F. A. Williams, "Some Aspects of Structures of Turbulent Pool Fires," Fire Technology, Vol. 15, No. 2, May 1979.

Harsha, P. T., W. N. Bragg and R. B. Edleman, "Preliminary Report: Improvement of a Mathematical Model of a Large Open Fire," NASA CR-152388, Science Applications, Inc., Contract # NAS2-10327, 1980.

McCaffrey, B. J., "Purely Buoyant Diffusion Flames: Some Experimental Results," Eastern Section of Combustion Institute, November 1978, Miami Beach, Florida.

Nielsen, H. J. and F. N. N. Tao, "The Fire Plume Above A Large Free-Burning Fire," 10th Symposium (International) on Combustion, p. 965-72, The Combustion Institute, Pittsburg, 1965.

Steward, F. R., "Prediction of the Height of Turbulent Diffusion Buoyant Flames," Comb. Sci. Tech., Vol. 2., pp. 203-212, 1970.

Thomas, P. H., "The Size of Flames from Natural Fires," 9th Symposium (International) on Combustion, pp. 844-59, Academic Press, New York, 1963.

APPENDIX A

Theory of the Vane Anemometer

The vane anemometer consists of a small vane wheel mounted on bearings which are made as frictionless as possible. If the resistance to rotation of the wheel were strictly zero and the incident flow over the anemometer region were uniform, each vane would move such that the fluid reaction in it was zero. This would imply that the relative velocity of the fluid and vane along the normal to the vane was zero. If the plane of the vanes make an angle Θ with respect to plane of rotation, then the component of the free stream velocity and rotational velocity normal to the vane surface are as follows

$$\left.\begin{array}{l}\text{Component of free stream velocity: } U_\infty \cos\theta \\ \text{Component of rotational velocity: } \omega R \sin\theta\end{array}\right\} \quad (1)$$

where ω is the rotational speed, R is the radius and U_∞ is the free stream velocity. Equating both components in (1), we obtain

$$\omega = U_\infty \frac{\cot\theta}{R} \quad (2)$$

Hence, ω is dependent only on the free stream velocity and the twist angle and is independent of the stream fluid density.

A similar result can be deduced using the Air-Screw theory. The power generated by a wind mill is given by the following expression

$$P = 0.5\,\eta\,\pi R^2 \rho U_\infty^3 \quad (3)$$

where η = efficiency of the machine

ρ = density of the medium

The power is also equal to

$$P = 2\pi\omega R Q \tag{4}$$

where Q is the torque force acting on the vane and is given by the following equation

$$Q = L \sin\theta + D \cos\theta$$

The lift, L and Drag, D forces acting on the vane surface can be obtained using the following expression

$$\left.\begin{aligned} L &= \frac{1}{2}\rho C_L S \left(U_\infty^2 + (2\pi R\omega)^2\right) \\ D &= \frac{1}{2}\rho C_D S \left(U_\infty^2 + (2\pi R\omega)^2\right) \end{aligned}\right\} \tag{5}$$

where S is the total surface area of the vanes. Hence, the power generated is given by

$$P = 4\pi^3 \rho S \omega^3 R^3 \{C_L \sin\theta + C_D \cos\theta\}(1+\mu^2) \tag{6}$$

where μ is the advance ratio defined as follows

$$\mu = U_\infty / 2\pi R\omega \qquad (7)$$

Equating equations (3) and (6), we find that the rotational speed ω is dependent linearly on the free stream velocity and is independent of the density of the media.

APPENDIX B

Thermophysical Properties of JP-4 Fuel

In making the calculations indicated in this report several JP-4 and other property values were utilized. These are indicated below:

Property	Value	Units
Density of liquid	770	kg/m^3
Flash point	340	K
Boiling point	520	K
Heat of vaporization	3.3×10^5	J/kg
Heat of combustion	4.65×10^7	J/kg
Density of air at STP	1.2	kg/m^3
Specific heat of air	10^3	J/kg K
Air fuel (mass) stoichiometric ratio	17	

1. Report No.	2. Government Accession No.	3. Recipient's Catalog No.
NASA CR-159209		

4. Title and Subtitle	5. Report Date
Analysis of NASA JP-4 Fire Tests Data and Development of a Simple Fire Model	April, 1980
	6. Performing Organization Code
7. Author(s)	8. Performing Organization Report No.
Phani Raj	81857-6
9. Performing Organization Name and Address	10. Work Unit No.
Arthur D. Little, Inc. 25 Acorn Park Cambridge, MA 02140	534-03-23-01
	11. Contract or Grant No.
	NAS1-15380
12. Sponsoring Agency Name and Address	13. Type of Report and Period Covered
National Aeronautics and Space Administration Washington, DC 20546	Contractor Report
	14. Sponsoring Agency Code

15. Supplementary Notes

Langley Technical Monitor: Dr. Wolf Elber
Ames Research Center Coordinator: Dr. Joseph Mansfield

16. Abstract

The temperature, velocity and species concentration data obtained during the NASA fire tests (3m, 7.5m and 15m diameter JP-4 fires) were analyzed. Utilizing the data analysis, a sample theoretical model was formulated to predict the temperature and velocity profiles in JP-4 fires. The theoretical model, which does not take into account the detailed chemistry of combustion, is capable of predicting the extent of "necking" of the fire near its base.

17. Key Words (Suggested by Author(s))	18. Distribution Statement
Fire testing Fire plume theory JP-4 fuel fire Carbon fiber risk assessment	Unclassified - Unlimited

19. Security Classif. (of this report)	20. Security Classif. (of this page)	21. No. of Pages	22. Price*
Unclassified	Unclassified	54	